COMMISSION OF EUROPEAN COMMUNITIES

NATIONAL TECHNICAL UNIVERSITY OF ATHENS
DIVISION OF WATER RESOURCES - HYDRAULIC AND MARITIME ENGINEERING

A F O R I S M:
A COMPREHENSIVE FORECASTING SYSTEM FOR FLOOD RISK MITIGATION AND CONTROL

ANNEX 1

PRESENTATION OF DATA COLLECTED FOR THE AFORISM PROJECT

by: I. Nalbantis and N. Mamassis

CONTRACT NO.: EPOC-CT90-0023
PROJECT COORDINATOR: PROF. E. TODINI
GROUP LEADER: PROF. TH. S. XANTHOPOULOS

ATHENS - JUNE 1992

Presentation of the data collected for the AFORISM project

By: I. Nalbantis and N. Mamassis
National Technical University of Athens
Division of Water Resources, Hydraulic and Maritime Engineering
5 Iroon Polytechniou, 15700, Zografou, Greece

CONTENTS

1. General

1.1. General situation of hydrologic data in Greece

The general situation of the hydrological data in Greece may be summarized as follows:

- The density or rain gauge network is satisfactory for operational purposes (in agreement with WMO standards).
- The flow measurement stations network depends on the specific needs of Greek authorities, and is mainly determined by planned works.
- There are several authorities responsible to perform hydrological measurements and to keep hydrological data files. The coordination between the authorities is not satisfactory.
- The reliability of measurements and data is poor in some cases, and better in other.
- The data in their majority are not processed. Charts of autographic instruments are not digitized nor tabulated.
- Although data exist, all the authorities with the exception of the Public Power Corporation (PPC), do not establish stage-discharge relationships for the river gauge stations. The most usual situation in the Greek rivers is that stage-discharge relationships are very unstable.
- Untill now all the work for data acquisition and preprocessing is performed manually. Data files are not yet stored in computers.
- Because of the above, the work required for any hydrological investigation is significantly increased due to the need for construction of reliable data sets.

1.2. The study area

The Evinos River Basin was selected among 3 possible basins as a study area for the following reasons:

The Evinos River Basin is situated in the West Sterea Hellas Water District and is surrounded by Panetolikon Mountain (N-NW), Vardoussia Mountains (NE), the Naupactus' Mountains (SE) and Arakinthos Mountain (W). The surrounding basins are: the Mornos River Basin from the East, the Sperchios River Basin from NE and from the North and West the Acheloos and Lake Trichonis basins (see Fig. 1). The most reliable stage recording station is located at Poros Riganiou with an upstream watershed area of 884 km^2 while the total basin area is 1129 km^2. An additional stage recorder has recently been installed at Neochori (349 km^2) near the site of the planned Ag. Dimitrios Dam which will serve the Athens water supply.

The elevations along the main water course range from 150 m.a.s.l. at Poros Riganiou to 1680 m.a.s.l. at the most upstream end, while the mean ground elevation upstream Poros Riganiou is 990 m. The main tributaries are: Kotsalos in the East and Fidakia and Gidomandritis in the West. Two basic geological formations prevail: limestone (51.4 %) especially in the central zone and flysch (48.6%). The mean annual flow at Poros Riganiou amounts 920 mm whereas the mean annual precipitation is 1463 mm (upstream the Perista dam site).

1.3 Discharge data

The water level is monitored at Poros Riganiou by the Public Power Corporation (PPC). There are 3 series of staff gauges and one float-type stage recorder while current metering is carried out with a frequency of 1/month. Continuous series of water level data together with current metering data are available for two periods: 28-4-61 to 17-11-63 (18 measurements) and 14-10-68 to 1987 (339 measurements).

Construction of the rating curves for the above periods has been done by the research group. This involves the following steps:

(a) Plotting of H-Q pairs on a log-log paper (H = water level, Q = discharge).
(b) Separating the points into subgroups that follow a relatively smooth line. This leads to separate rating curves for periods of application ranging from 1 to 7 months.
(c) Attaching to all identified rating curves the relatively rare data with large values of H and Q.
(d) Extrapolation of the rating curves through hydraulic methods based on approximate field data.
(e) Expression and storage of each rating curve as a series of a limited number of points on a log-log scale (30 points), thus avoiding restricting analytical expressions.

Based on the above method the research group identified 2 rating curves for the period 1961-63 and 15 for the period 1968-1987 in the framework of a project for the Athens Water Supply system study (Koutsoyiannis & Xanthopoulos, 1990). In order to be more realistic, one must also consider the following methodological improvements in order to increase the reliability of the dischagre data:

(a) Cross section field measurements and more accurate reconstruction of stage-discarge curves.
(b) Water level data correction to account for the discrepancies between measured and estimated discharges.

It is worthy to mention the most important recorded floods: on 3-12-76 the discharge rose from 400 m^3/s to 1676 m^3/s within 6 hour while on 30-12-70 the discharge increased from a few m^3/s to 1351 m^3/s.

1.4 Rainfall data

Three rainfall recording gauges are available in the broader area of the Evinos River Basin, as shown in the following table

Table 1. Recording raingauges in the Evinos River Basin

Station Name Code	*Period of operation*	*Elevation (m a.s.l.)*	*Coordinates (φ, λ)*	
Drymonas	1971-	900	38:38	21:40
Krikelo	1959-	1120	38:48	21:51
Aniada	1959-	1060	38:9	21:47

All stations are operated by the Public Power Corporation (PPC) and they are considered reliable. Only Drimonas is located inside the Evinos basin. The raw hourly data were extracted from the instrument tapes for a 20-year period (1970-1990). The data were entered into a regional

database. The extracted hourly time series were continous in time with very short periods of missing data. Interruptions of the gauge operation correspond to winter periods with frost or to periods with malfunctions of the instruments. Generally speaking the data are considered reliable. The data reliability was tested by constructing comparison plots of the three rainfall series. Some of these plots are depicted in Figures 2,3 and 4.

In addition to the hourly rainfall data, daily rainfall depths from non-recording raingauges were used. These data were collected and entered into a database within the framework of another project. The characteristics of the above gauges together with the period of operation are presented in the following table

Table 2 Non-recording Rain gauges in the Evinos River Basin.

Station Name	*Code*	*Period of operation*	*Elevation (m a.s.l.)*	*Coordinates (φ, λ)*	
Analipsi	405	1950-	620	38:30	21:42
Poros Righaniou	477	1960-	150	38:30	21:45
Drymonas	424	1970-	900	38:38	21:40
Platanos	475	1950-	900	38:36	21:47
Grammeni Oxia	420	1950-	1160	38:44	22:00
Grighorio	421	1951-1984	1000	38:38	21:59
Arachova	409	1960-	960	38:41	21:52

1.5 Meteorological data

Four station thermometers for air temperature measuremets exist within the Evinos River Basin. An estimate for mean daily temerature can be derived from these measurements. The stations together with their codes as shown in Fig. 1, are presented in the following Table.

Table 3 Temperature gauges in the Evinos River Basin

Station Name	*Code*	*Period of operation*	*Elevation (m a.s.l.)*	*Coordinates (φ, λ)*	
Arachova	409	1973-	960	38:41	21:52
Poros Righaniou	477	1973-82	150	38:30	21:45
Drymonas	424	1973-	900	38:38	21:40
Grammeni Oxia	420	1969-	1160	38:44	22:00

The data from Grammeni Oxia are not considered by the Public Power Corporation (PPC) to be reliable. As a result, the other 3 stations were used in the AFORISM project. The areal daily mean temperature for the whole basin was calculated as follows: Estimates of the daily mean temperature at the average elevation of the basin are made first based on the point daily mean temperature from each station and the observed lapse rate. Then the arithmetic mean of these estimates is calculated.

2. Data preparation for rainfall-runoff analysis

2.1 Continuous series

A continuous series of hydrological variables was constructed in order to test different rainfall-runoff models. This series covers a 2-year period from October 1979 to September 1981. This period was chosen for the following reasons: (i) it contains significant flood events which allow the fast response components of any rainfall-runoff model to be activated and (ii) there is no significant snowfall. The last condition allows us to test different models without the inclusion of a snowmelt submodel. The data set consists of the following variables:

- Hourly areal rainfall depth in mm
- Hourly discharge in m^3/s
- Daily areal temperature in ^oC.

Some observed hydrographs and hyetographs on an hourly basis are shown in figures 5 and 6 for 1-month periods.

2.2 Event-based data

A set with event-type data was constructed in order to calibrate event-type rainfall-runoff models. Flood events covering the period 1974-1988 were selected based on the following criteria: (i) there exists a significant variation in measured water levels within a short period of time (ii) there is no significant snowfall recorded in the raingauges; (this was the reason we have excluded all late winter floods) and (iii) there are no missing data or any other problems in the rainfall records.

Finally, 28 flood events were chosen. These events are presented in the following table.

Table 3 Flood events selected in the Evinos River Basin

Event number	*Duration (hours)*	*Start*
1	120	1973-12-14
2	144	1974-10-20
3	216	1974-10-27
4	96	1975-12-18
5	120	1976-12-02
6	96	1976-12-06
7	144	1976-10-31
8	120	1978-12-13
9	96	1979-01-01
10	144	1979-01-11
11	240	1979-01-24
12	216	1980-12-04
13	120	1980-11-09
14	168	1980-11-28
15	72	1981-12-07
16	144	1981-12-12
17	192	1981-12-22
18	72	1981-10-27
19	168	1982-12-10
20	96	1982-12-17

Table 3 Flood events selected in the Evinos River Basin (Continued)

Event number	*Duration (hours)*	*Start*
21	192	1982-11-14
22	96	1984-01-10
23	120	1984-11-18
24	192	1985-11-01
25	168	1985-11-19
26	168	1985-11-25
27	120	1988-11-20
28	120	1988-11-24

The observed hydrographs for 4 flood events are depicted in Figures 7 and 8. The corresponding hyetographs of areal rainfall are also shown in the same Figures.

3. Data preparation for the analysis of intense rainfall

3.1 Criteria for the identification of isolated storms

Two different criteria were used to seperate the rainfall events, based on either the meteorological conditions (succession of weather types) or on the statistical properties of the rainfall process (time duration between events). To develop and apply the first criterion it is necessary to examine weather maps, determine the successive weather types and seperate the rainfall produced by each type. The second criterion it is sufficient to examine the rainfall process in time, find the common dry period in the different rain recorders and consider a threshold for the seperation time between two events. A value of 8-12 hours was considered as a reasonable estimate of this threshold for the study area. Comparison plots of the rainfall records in time for different stations such as the ones in Figures 2-4 are helpful for the identification of seperate storm events.

3.2 Criteria for the selection of intense rainfall event

From the continuous records of rainfall the most severe events were chosen to be studied in detail. The selection of those intense rainfall events was made by using threshold levels for both the daily and hourly depths. These threshold levels were selected so as to have a sufficient number of events. The selected values of the levels were 25 and 7 mm for the daily and hourly depths respectively. Based on those values, a record of more than 250 events was extracted from a 20 year period for three rain recorder stations in Evinos River Basin.

3.3 Classification of events by weather type

A classification introduced by Maheras [1982] for weather types in Greece was initially used. Maheras examined weather maps at the surface and at the 500 mb level and defined five anticyclonic, six cyclonic, two mixed and three special weather types that affect the East Mediterranian territory. The orbits of cyclones and anticyclones, the place of their genesis and the meteorological conditions at the 500 mb levels were the main characteristics for weather type definitions. He also made a calendar of the weather type of each day for a thirty year period (1960 - 1990). Two of the above cyclonic weather types (SW1, NW1) and one special weather type

(DOR) produce the main amount of rainfall in Greece. The other four cyclonic types produce rainfall in smaller amounts. Using this calendar the events of the constructed record of the Evinos River Basin were classified as follows:

SW1	33%
NW1	28%
W1	10%
W2	5%
SW2	8%
NW2	8%
DOR	8%

More precice classification is scheduled for the future in order to include the action of other meteorological patterns such as fronts, sectors and air mass movements.

References

Maheras P., *Synoptic conditions and multi-variate analysis of weather in Thessaloniki*, Laboratory of Climatology, University of Athens, 1982

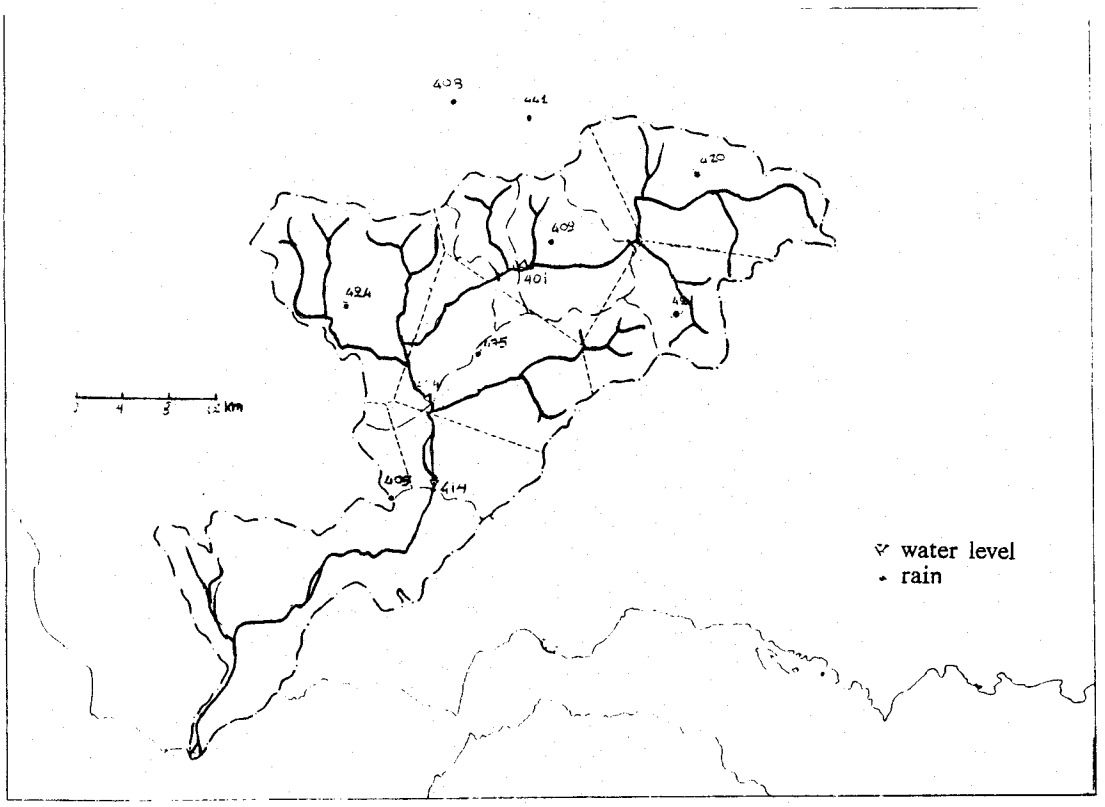

Fig. 1 The Evinos River Basin

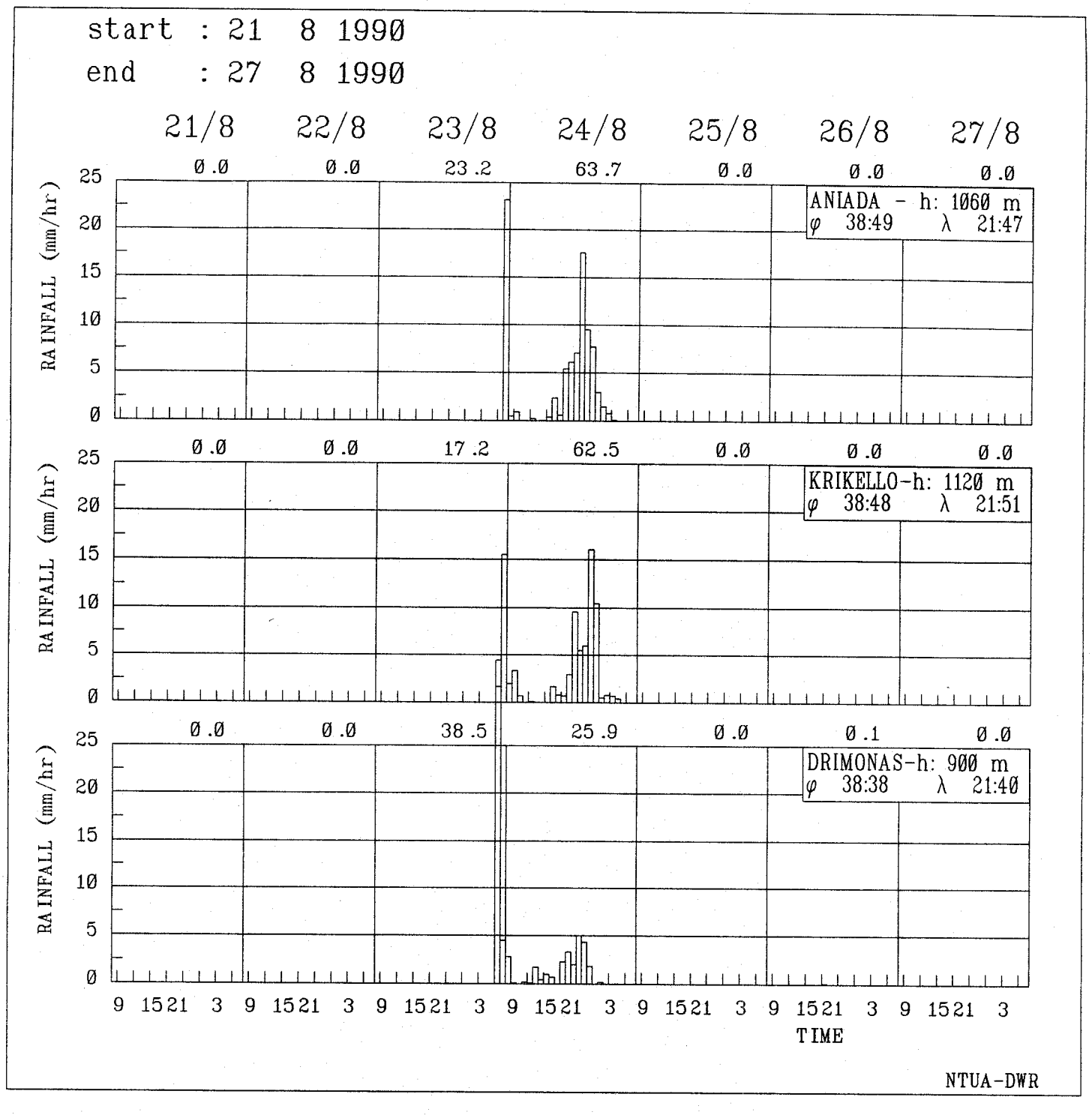

Fig. 2 Comparison plots for hourly point rainfall intensities

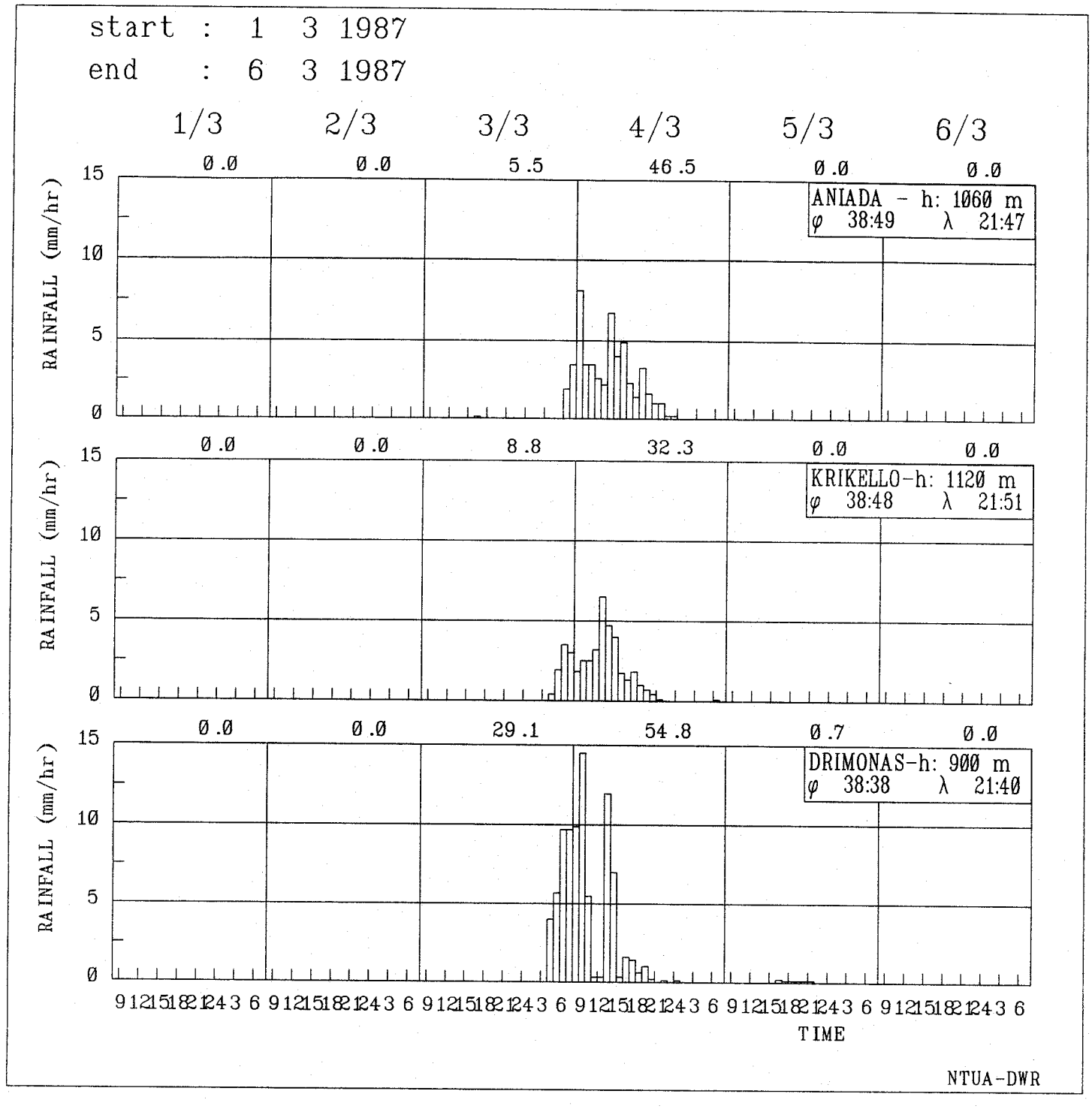

Fig. 3 Comparison plots for hourly point rainfall intensities

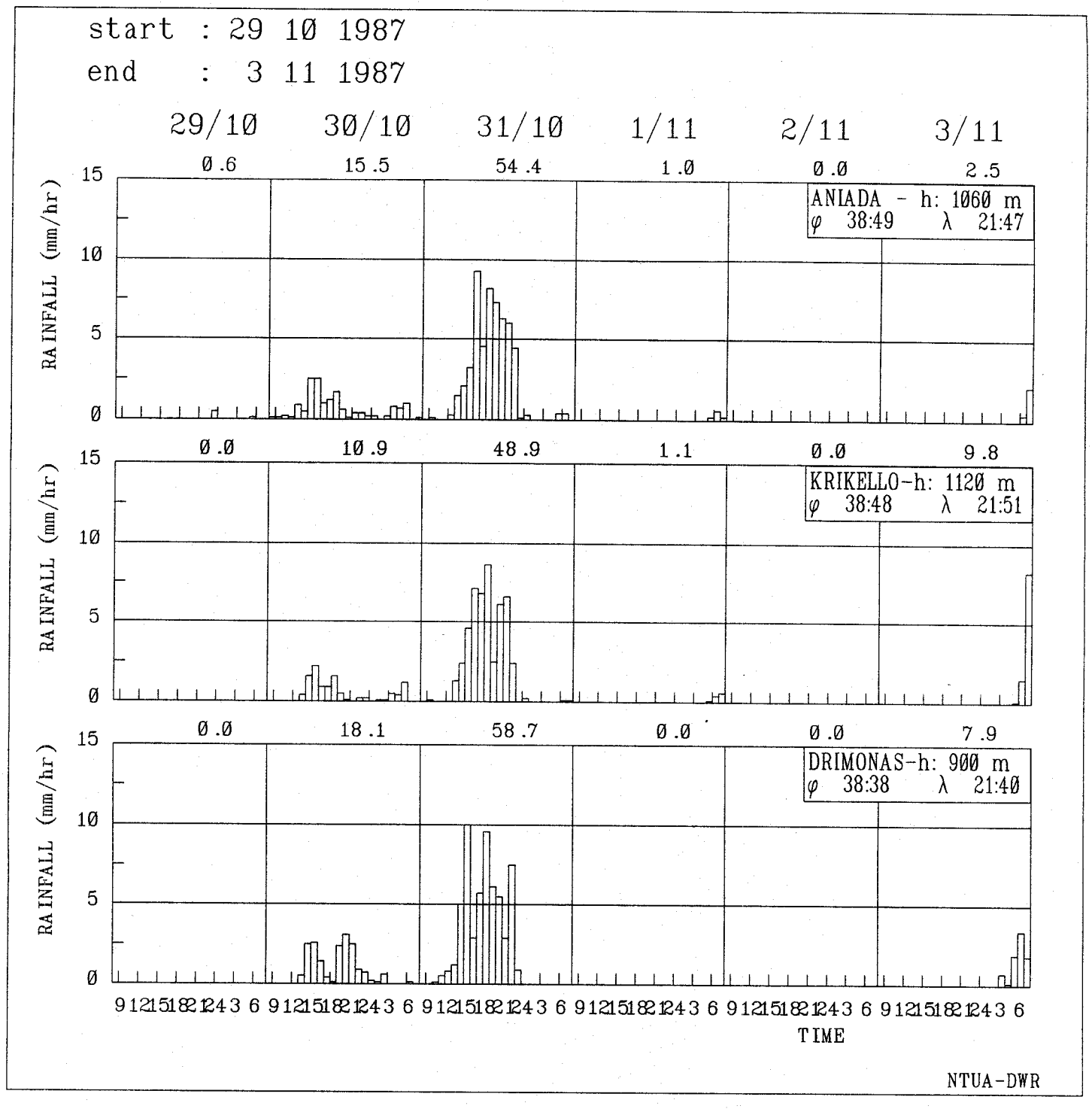

Fig. 4 Comparison plots for hourly point rainfall intensities

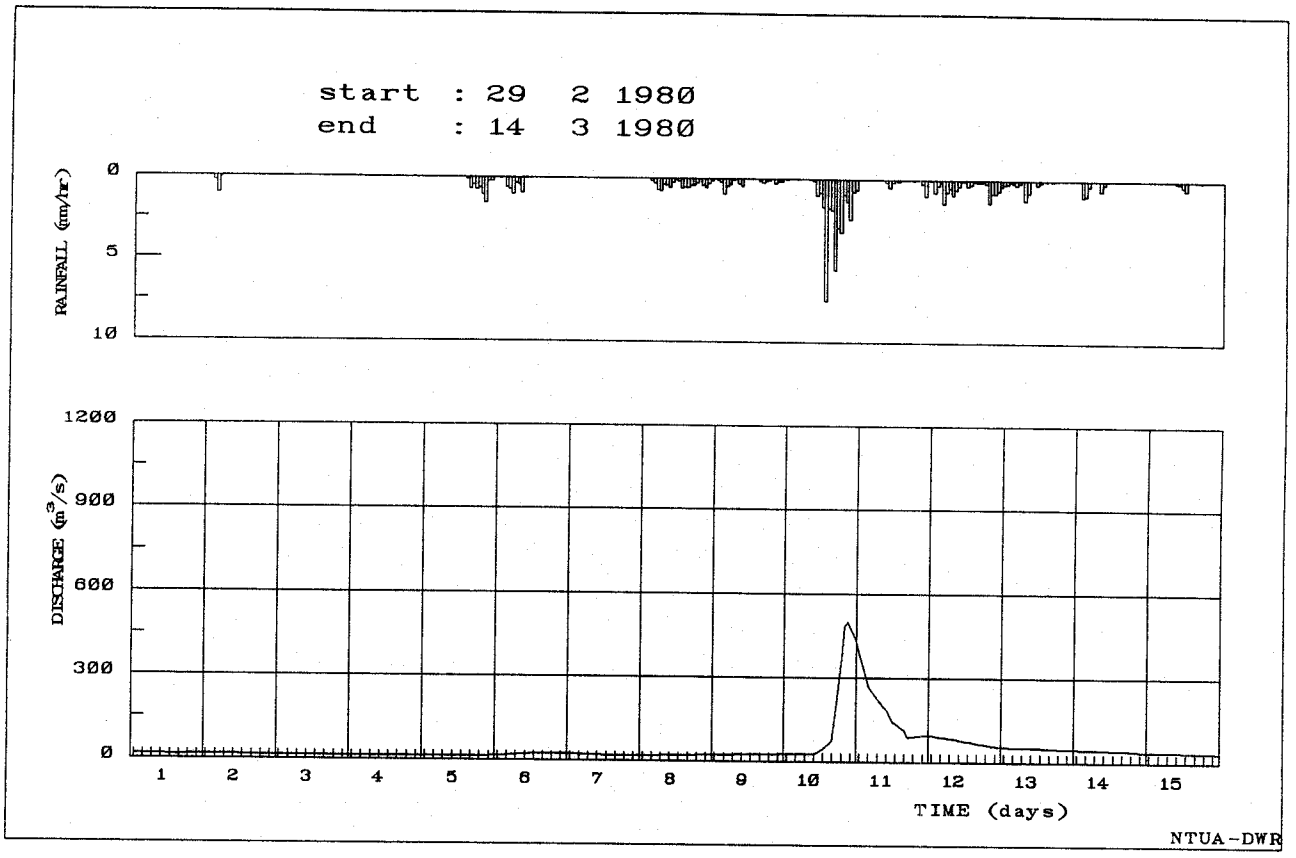

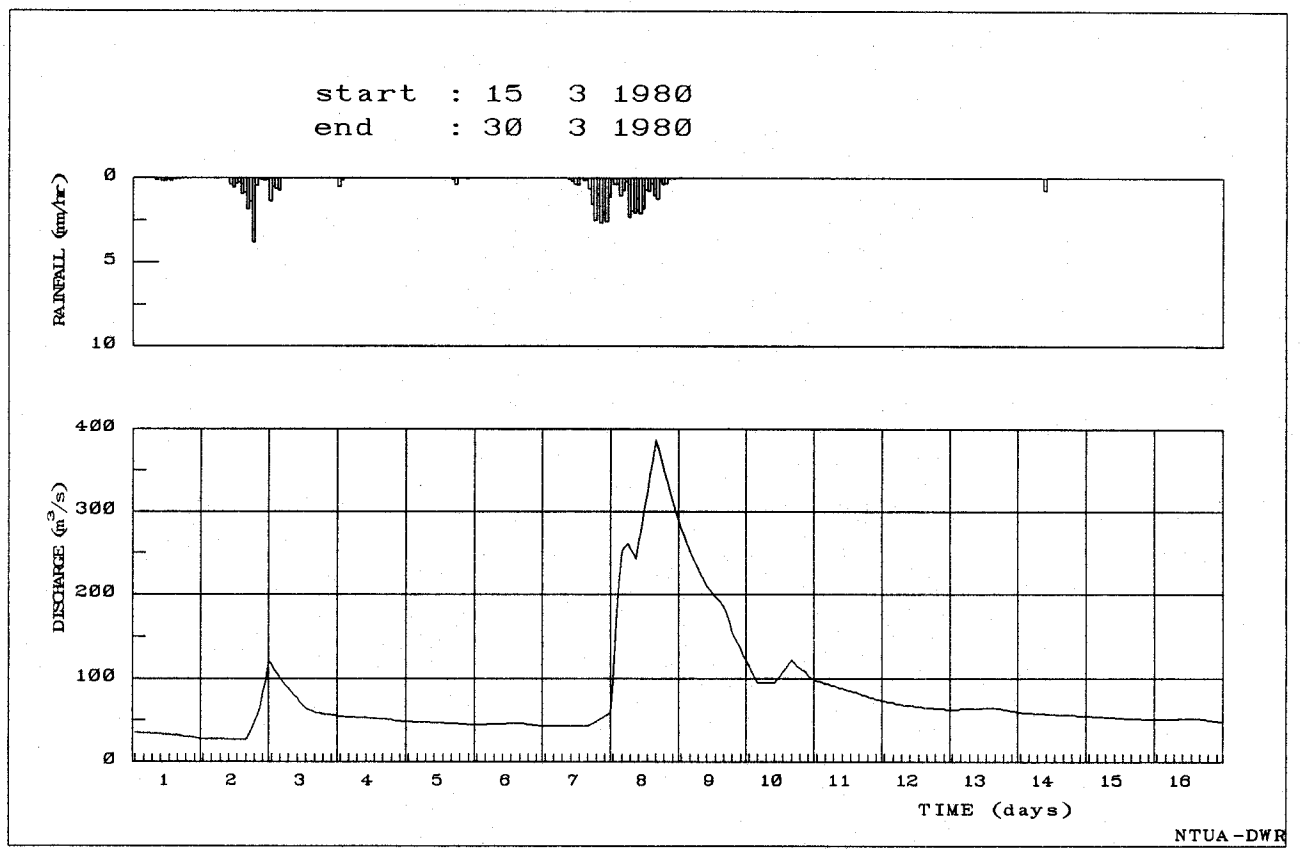

Fig. 5 Hourly rainfall-runoff data on a continuous time basis

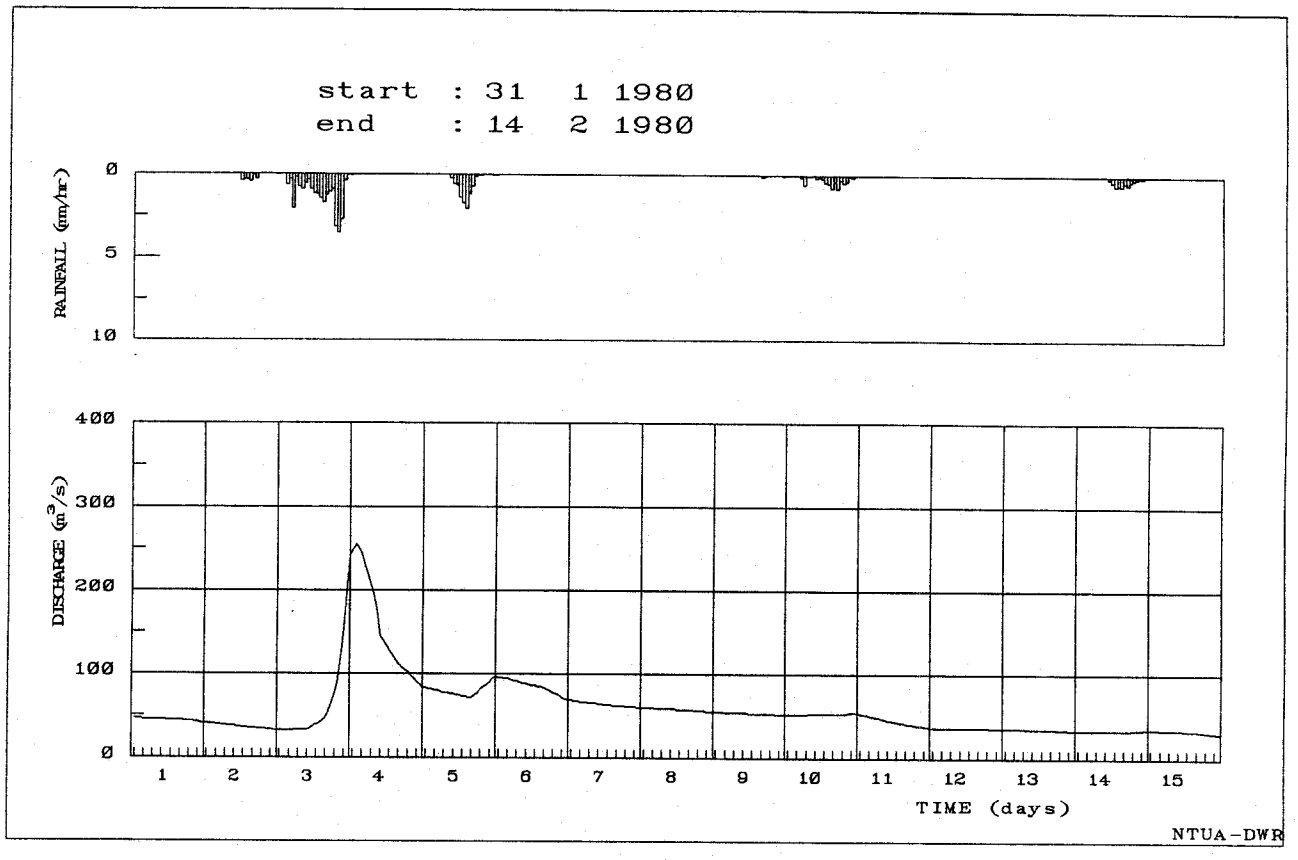

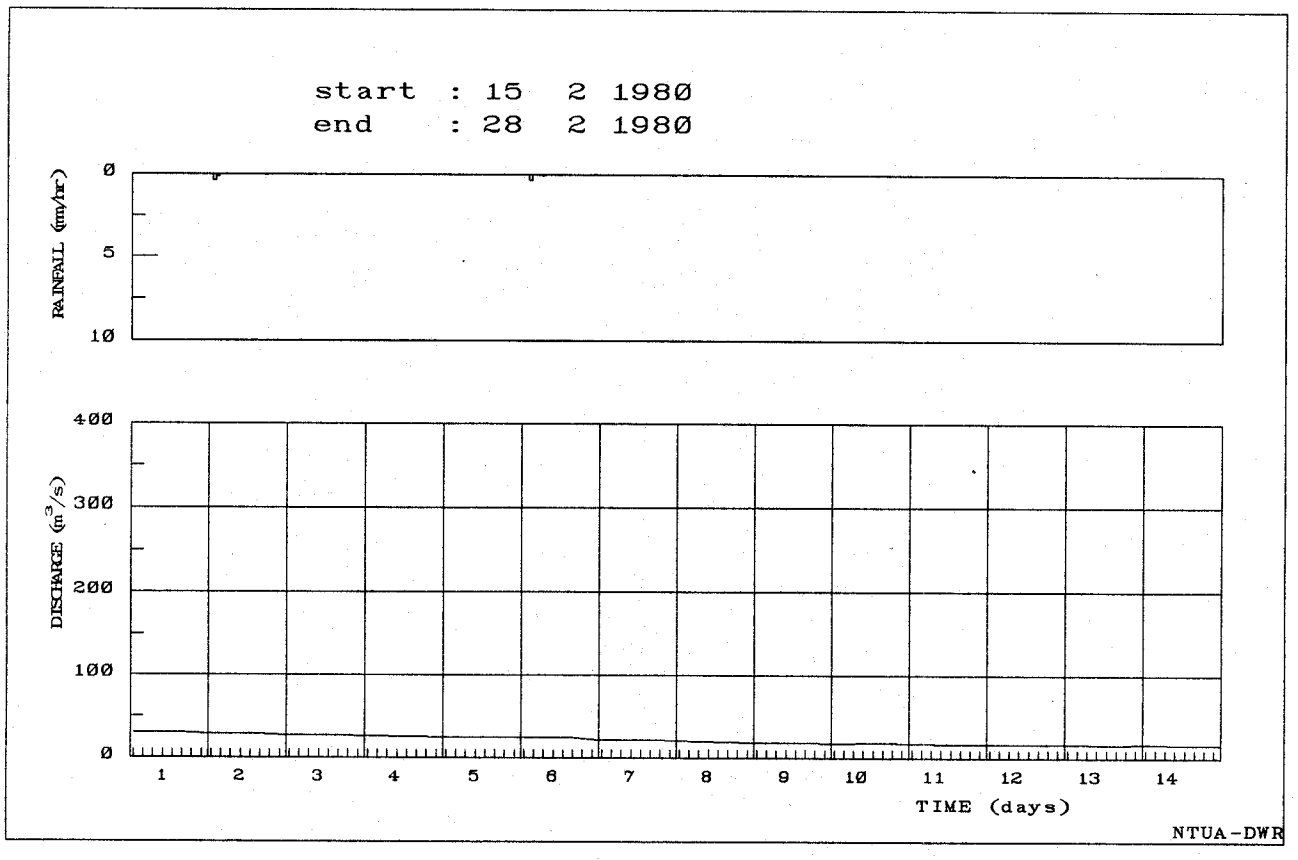

Fig. 6 Hourly rainfall-runoff data on a continuous time basis

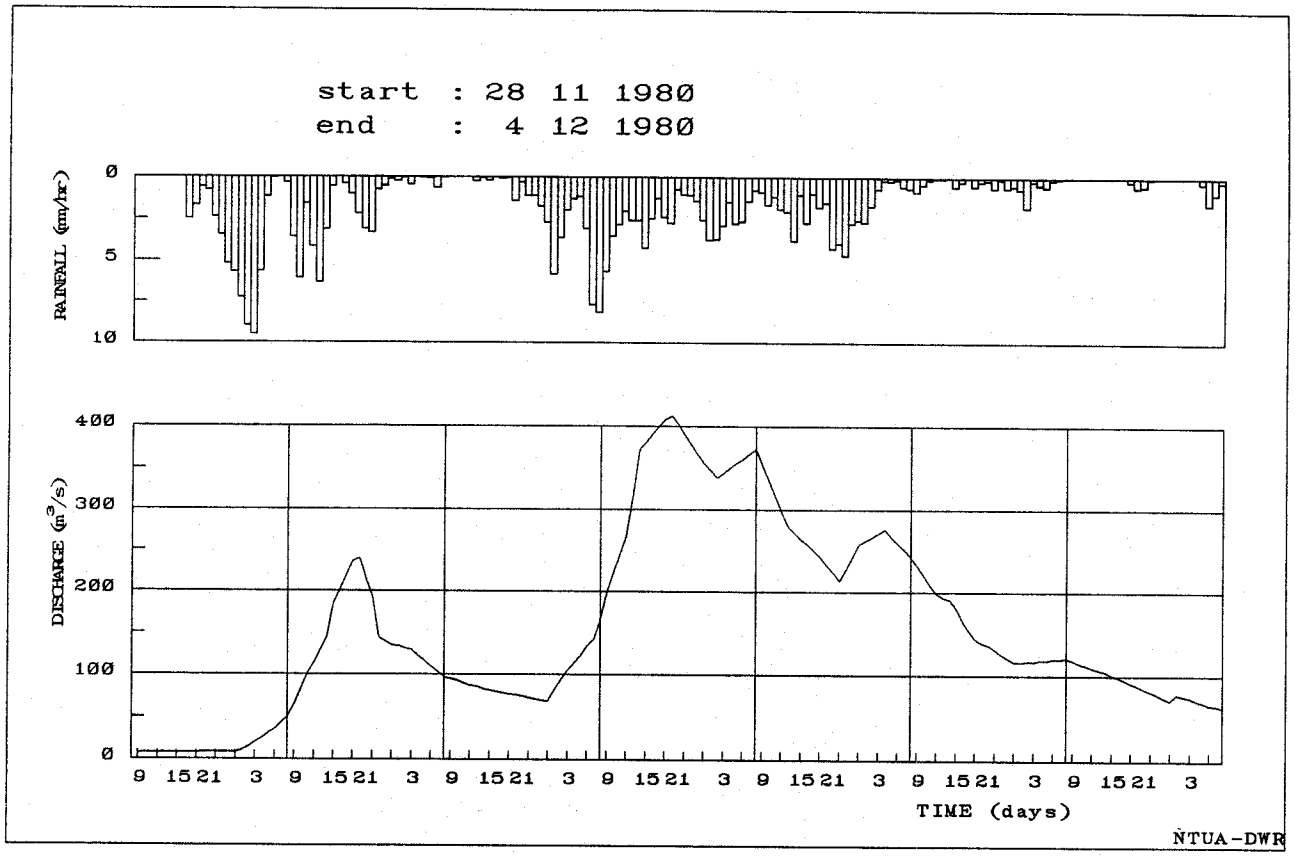

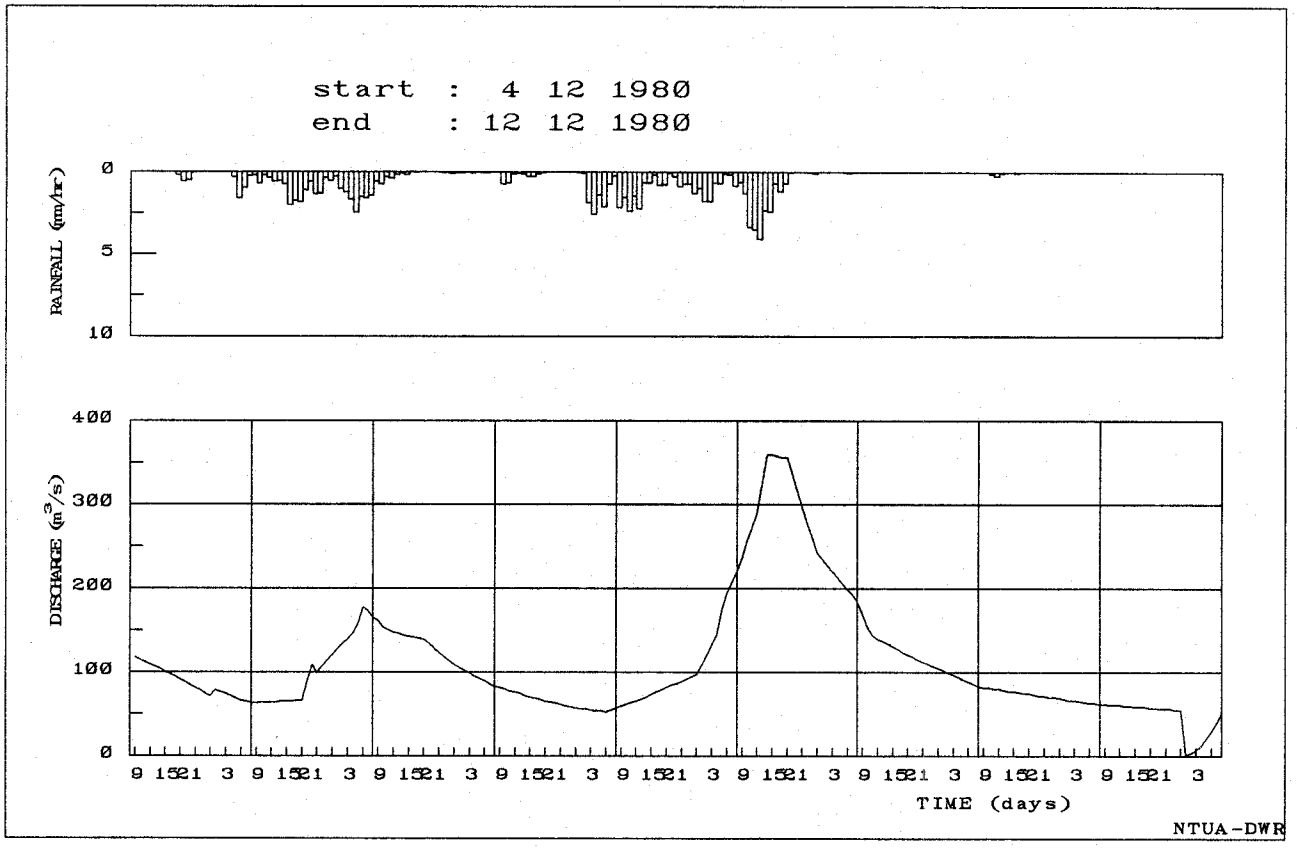

Fig. 7 Hourly rainfall-runoff data on an event basis

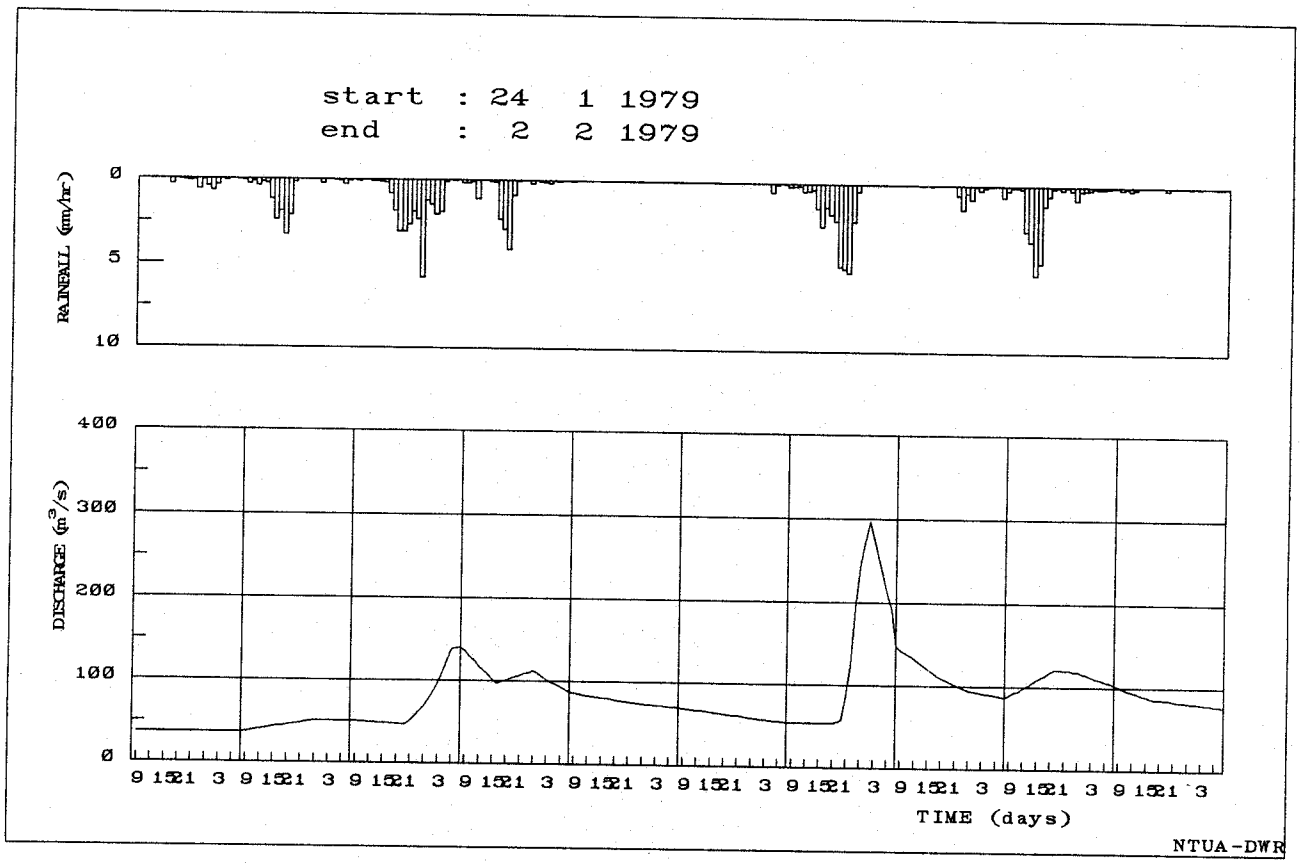

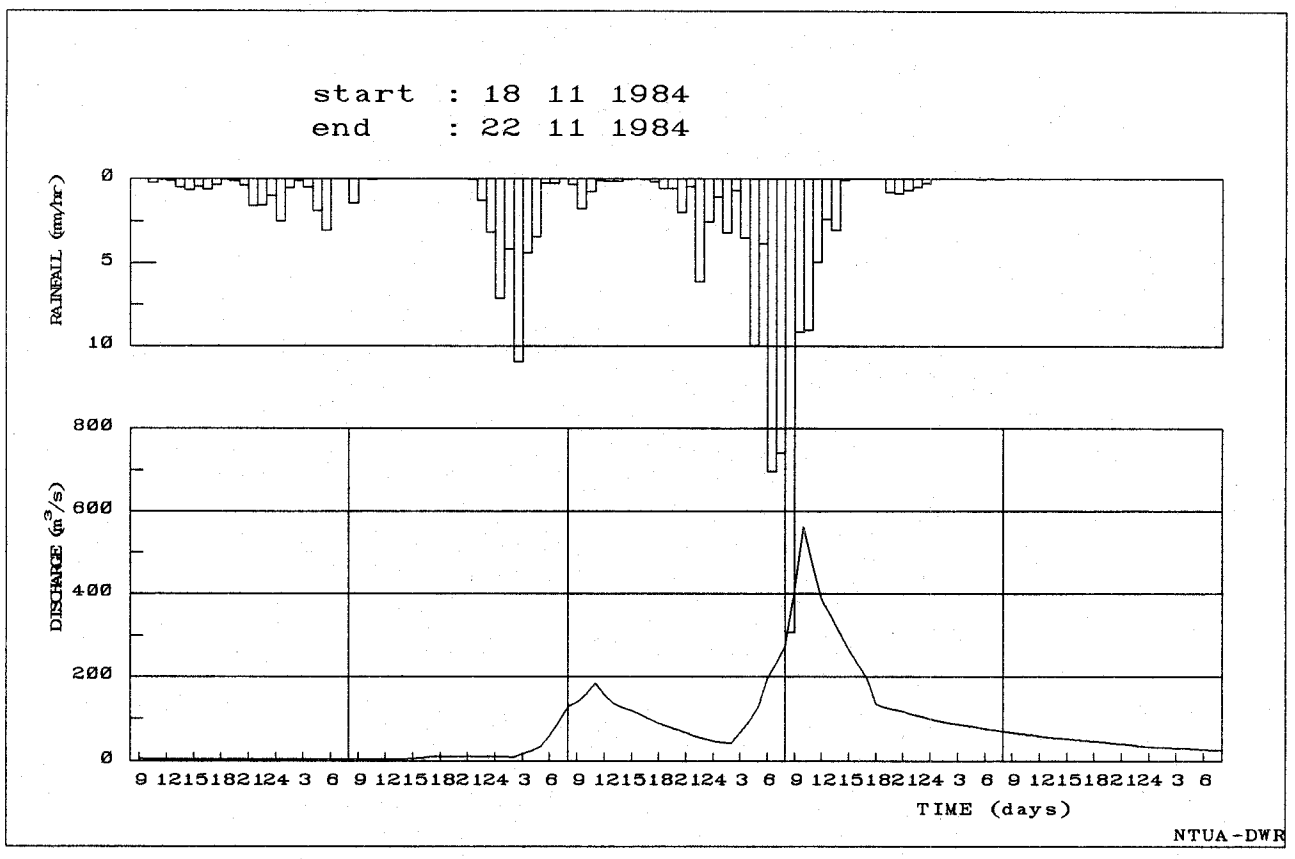

Fig. 8 Hourly rainfall-runoff data on an event basis

COMMISSION OF EUROPEAN COMMUNITIES

NATIONAL TECHNICAL UNIVERSITY OF ATHENS
DIVISION OF WATER RESOURCES - HYDRAULIC AND MARITIME ENGINEERING

A F O R I S M:
A COMPREHENSIVE FORECASTING SYSTEM FOR FLOOD RISK MITIGATION AND CONTROL

ANNEX 2

RAINFALL-RUNOFF MODELING IN A MEDITERRANEAN ENVIRONMENT

by: I. Nalbantis

CONTRACT NO.: EPOC-CT90-0023
PROJECT COORDINATOR: PROF. E. TODINI
GROUP LEADER: PROF. TH. S. XANTHOPOULOS

ATHENS - JUNE 1992

Rainfall-runoff modeling in a Mediterranean environment

by Ioannis Nalbantis

National Technical University of Athens

Division of Water Resources, Hydraulic and Maritime Engineering

5 Iroon Polytechniou 15700, Zografou, Greece

CONTENTS

1. INTRODUCTION

Modern flood forecasting systems require, among other components, reliable and accurate rainfall-runoff models. The identification of these models necessitates high quality and adequate quantity data. The problem of data adequacy becomes more severe in southern European countries where the establishment of modern hydrologic networks has had a considerable delay. The existence of recording devices cannot be guaranteed in many river basins. Inversely, one can easily find a rather huge amount of daily data from non-recording devices e.g. staff readings. The calibration of any rainfall-runoff model at early stages of the forecasting system operation has to be based on a very short record coming from a newly built data collection system and ignore the old data that seem inadequate. The problem under investigation is to examine the possibility of extracting information from daily data and using it within a short time step rainfall-runoff model. We expect that this extra information may enhance the performance of the model.

Suppose that we need hourly data for our rainfall-runoff model. We may conceive the following framework for model testing:

1. Calibration of an hourly rainfall-runoff model on a short continuous-time data record (record 1).
2. Verification of the same hourly rainfall-runoff model on a short continuous-time data record (record 2).
3. Calibration of a daily rainfall-runoff model, having the same structure with the hourly model, on a relatively long continuous-time data record (record 3).
4. Verification of the above daily rainfall-runoff model on a relatively long continuous-time data record (record 4).
5. Use, within the hourly model, of some parameters of the daily model either directly or after transformation and verification on record 2.
6. Comparison of results
7. Extension to other models.

We have chosen SACRAMENTO model (Burnash et al., 1973) as the first model to test because this model has been applied widely and has inspired many other models. Also, it has been systematically compared to other models (see Franchini and Pacciani, 1989, 1991). The behavior of the model concerning its identifiability has also been extensively studied (Gupta and Sorooshian, 1981, Sorooshian and Gupta, 1983a, Sorooshian and Gupta, 1983b, Gupta and Sorooshian, 1985, Sorooshian and Gupta, 1985). In this report we present results

on the calibration and validation of this model for daily data of a Greek basin. This work corresponds to steps 3 and 4 described above. Note that these steps are totally independent from steps 1 and 2.

2. DESCRIPTION OF THE MODEL

The structure of the SACRAMENTO model is shown in Fig. 1. The basin's soil consist of two zones: the Upper Zone and the Lower Zone. Each zone has a tension water storage and a free water storage. The free water storage of the Lower Zone is further subdivided into two storages: the primary and the supplementary.

The area of the basin is split into two parts: the first which is impervious and the second which is pervious. Any precipitation reaching the impervious part is transformed to direct runoff. Precipitation on the pervious part of the basin follows a rather complex route through the 5 storage elements of the model. First, the Upper Tension Water Storage is filled and subsequently the excess water is accumulated in the Upper Zone Free Water storage. A portion of the content of the latter reservoir is depleted every time step thus producing interflow; if, in addition, the reservoir capacity is exceeded, excess water forms surface runoff.

Water from the Upper Zone Free Water percolates into the lower zones before interflow and surface runoff production. The rate of percolation depends on the water contents of both the Upper and the Lower Zone storages. The model introduces the concept of percolation demand of the Lower Zone *LZPD*. The minimum demand *PBASE* corresponds to the saturation of the Lower Zone when it equals the rate of depletion of the Lower Zone Free Water reservoirs. Analytically we can write

$$PBASE = (LZFSM \times LZSK) + (LZFPM \times LZPK) \qquad (1)$$

where

LZFPM and *LZFSM* are the capacities of the Primary and Supplementary Lower Zone Free Water respectively, and

LZPK and *LZSK* are the depletion coefficients of the Primary and Supplementary Lower Zone Free Water respectively.

During an extremely dry period when the Lower Zone storages are entirely empty we admit a

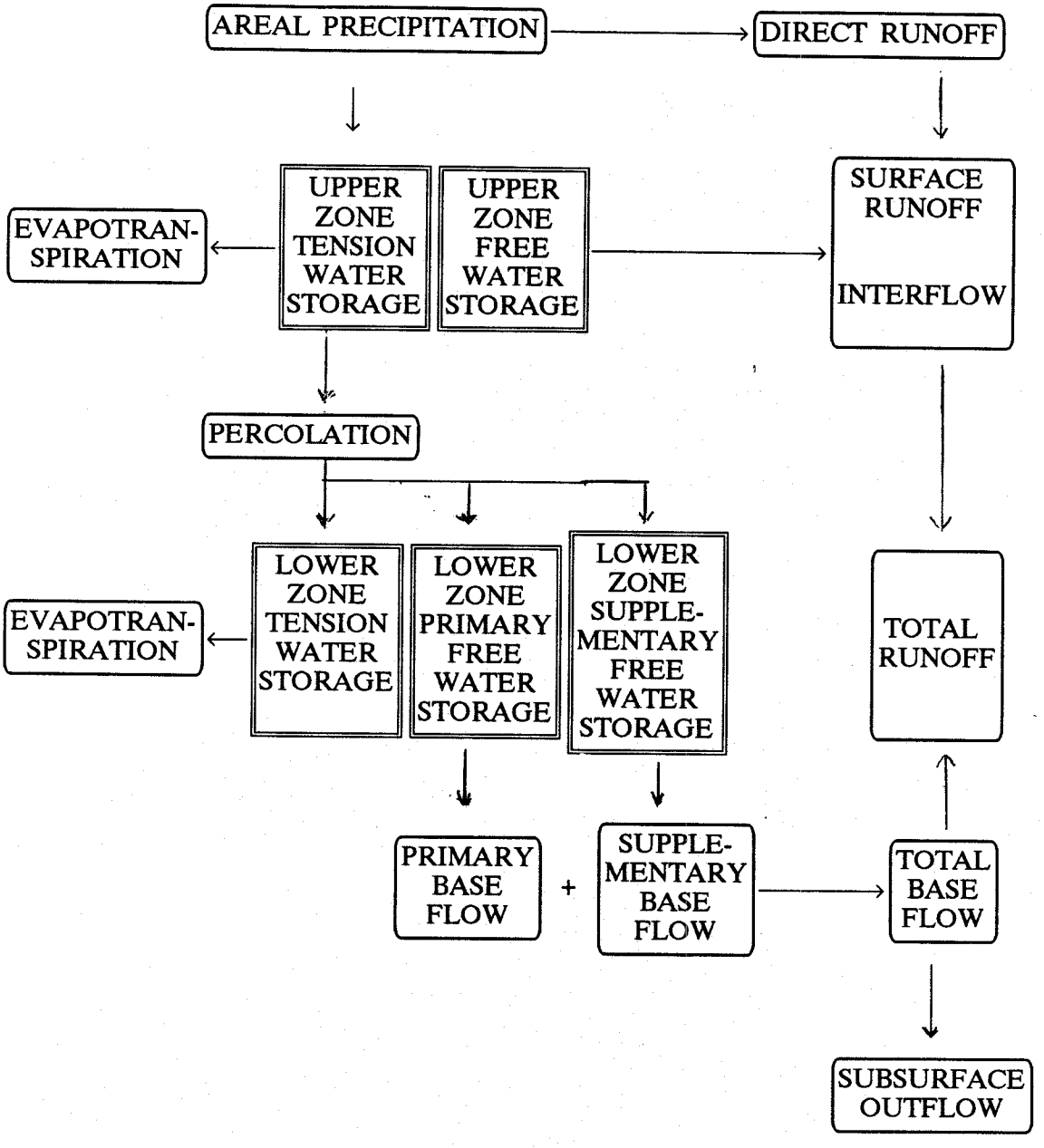

Figure 1. Schematic presentation of the SACRAMENTO model

percolation rate Z times greater than $PBASE$ that is $PBASE(1+Z)$. Generally speaking percolation demand is obtained by a non-linear interpolation between the above extreme values

$$LZPD = PBASE\left(1 + Z\, f\left(\frac{\Sigma \text{ Lower Zone deficits}}{\Sigma \text{ Lower Zone capacities}}\right) \right) \qquad (2)$$

The function f is given by

$$f = \left(\frac{\Sigma \text{ Lower Zone deficits}}{\Sigma \text{ Lower Zone capacities}} \right)^{REXP} \qquad (3)$$

where $REXP$ is a model parameter.

The actual percolation rate $PERC$ depends also on the availability of water in the Upper Zone Free water reservoir as follows

$$PERC = LZPD \frac{UZFWC}{UZFWM} \qquad (4)$$

The water volume which percolates, first fills tension water requirements before it appears as free water in the two Lower Zone Free water storages. This ideal behavior would indeed correspond to a vertical soil column in a laboratory. Spatial variability of soil properties and precipitation inputs in the catchment scale cause a deviation from the above behavior. The model assumes that a portion $PFREE$ of the percolating water volume enters directly the Lower Zone Free Water reservoirs. Distribution of water between the Lower Zone Free Water storages is made according to their relative deficits. The model does not permit the relative deficit (content/capacity) of the Lower Zone Tension Water storage to be greater than that of the Lower Zone Free Water storages. Should this happen, a transfer of water into the tension storage takes place in order to balance the difference of relative deficits. A portion of free water defined as the parameter $SAVED$ is exempted from this transfer.

The groundwater flow $QBASE$ from Lower Zone Free Water reservoirs is given by

$$QBASE = (LZFSC \times LZSK) + (LZFPC \times LZPK) \qquad (5)$$

where

LZFPC and *LZFSC* are the water contents of the Primary and Supplementary Lower Zone Free Water respectively.

The model accounts also for the subsurface outflow which is not observed at the basin's outlet. The parameter *SIDE* is defined to be the ratio of the outflow to the actually observed baseflow at the outlet.

The runoff appears in the following 5 forms

= **Direct runoff** from permanently or provisionally impervious parts of the basin.
= **Surface runoff** from Upper Zone Free Water storage when precipitation rate exceeds the sum of the rates of percolation and interflow.
= **Interflow** due to lateral drainage of the Upper Zone Free Water storage.
= **Supplementary baseflow.**
= **Primary baseflow.**

Evaporation from areas covered by water and riparian vegetation occurs at its potential rate

$$E_3 = ED\ SARVA \tag{6}$$

where

SARVA is the portion of the basin covered by water or riparian vegetation,
E_3 is evapotranspiration, and
ED is potential evapotranspiration.

The evapotranspiration from Upper Zone Tension Water storage is given by

$$E_1 = ED \frac{UZTWC}{UZTWM} \tag{7}$$

where

E_1 is evapotranspiration from the upper zone,
UZTWC is the soil moisture content of the upper zone,
UZTWM is the maximum soil moisture content of the upper zone, and
ED is potential evapotranspiration

The evapotranspiration demand from the Lower Zone Tension Water storage is equal to the remaining unsatisfied evapotranspiration demand ED - E_1. The actual evapotranspiration from the lower zone is

$$E_2 = (ED - E_1)\frac{LZTWC}{UZTWM+LZTWM} \quad (8)$$

where E_2 is evapotranspiration from the lower zone,

LZTWC is the content of the Lower Zone Tension Water storage, and

LZTWM is the capacity of the Lower Zone Tension Water storage.

In the next paragraphs we present the model inputs, the model parameters and other intermediate variables.

a. Inputs of the model

a1. Time series of daily rainfall depths (mm)

a2. Time series of daily potential evapotranspiration values (mm).

b. Parameters of the model

b1. Percentage of basin's area which is permanently impervious *PCTIM*

b2. Maximum percentage of basin's area which can be provisionally impervious *ADIMP*

b3 Percentage of basin's area covered by water and riparian vegetation *SARVA*

b4. Capacity of the Upper Zone Tension Water storage *UZTWM* (mm)

b5. Capacity of the Upper Zone Free Water storage *UZFWM* (mm)

b6. Depletion coefficient of the Upper Zone Free Water storage *UZK* (% of the content per time step)

b7. Capacity of the Lower Zone Tension Water storage *LZTWM* (mm)

b8. Capacity of the Upper Zone Primary Free Water storage *LZFPM* (mm)

b9. Capacity of the Upper Zone Supplementary Free Water storage *LZFSM* (mm)

b10. Depletion coefficient of the Lower Zone Primary Free Water storage *LZPK* (% of the content per time step)

b11. Depletion coefficient of the Lower Zone Primary Free Water storage *LZSK* (% of the content per time step)

b12. Percentage of increase of percolation demand from saturation to dryness *Z*

b13. Exponent of equation (3), *REXP*

b14. Percentage of percolating water entering directly lower zone free water storages *PFREE*

b15. Percentage of lower zone free water not available for evapotranspiration *SAVED*

b16. Ratio of subsurface outflow or loss to the observed base flow *SIDE*

c. Intermediate variables

c1. Percentage of impervious areas of the basin *ACTIM*

c2. Content of the Upper Zone Tension Water storage *UZTWC* (mm)

c3. Content of the Upper Zone Free Water storage *UZFWC* (mm)

c4. Content of the Lower Zone Tension Water storage *LZTWC* (mm)

c5. Content of the Lower Zone Primary Free Water storage *LZFPC* (mm)

c6. Content of the Lower Zone Supplementary Free Water storage *LZFSC* (mm)

Outputs of the model are

- Time series of total runoff
- Time series of runoff components
- Time series of intermediate variables
- Mean water balance for the whole period of application
- Numerical criteria on model performance

The numerical criteria of model's performance that have been implemented are:

Percentage of explained variance *EV* given by

$$EV = 1 - \frac{Vare}{VarQ} \tag{9}$$

where *VarQ* id the variance of measured discharge described below, and

Vare is the variance of the model residuals described below.

Vare is given by

$$Vare = \frac{1}{N} \sum_{i=1}^{N} \left((Q_i - QC_i) - (\bar{Q} - \overline{QC}) \right)^2 \tag{10}$$

where Q_i and QC_i are respectively the measured and estimated discharge for time i,

$\bar{Q}$ and $\overline{QC}$ are respectively the mean values of the measured and estimated discharge, and N is the length of the period of the model's application.

VarQ is given by

$$VarQ = \frac{1}{N} \sum_{i=1}^{N} (Q_i - \bar{Q})^2 \tag{11}$$

Efficiency of the model *EFF*, given by

$$EFF = 1 - \frac{MSE}{VarQ} \tag{12}$$

where *MSE* is the mean square error of the model residuals estimated by

$$MSE = \frac{1}{N} \sum_{i=1}^{N} (Q_i - QC_i)^2 \tag{13}$$

3. RESULTS

The SACRAMENTO model was applied to a 9-year continuous series of rainfall, runoff and evaporation data. The Evinos River Basin, lying in the West Sterea Hellas Water District (see Fig. 2) was the test basin. Water level data at Poros Righaniou were collected, digitized and processed to give reliable discharges. The watershed area is 884 km^2 with an average elevation of +990 m. On the map of Fig. 2 we show the 6 rain gauges and their codes used in our study: Poros Righaniou (414), Drymonas (424), Platanos (475), Arachova (409), Analipsi (405), Grighorio (421). The mean monthly temperatures were calculated based on 3 thermometers at the stations Arachova, Drymonas and Poros Righaniou. The model was calibrated manually based on the 1980-81 to 1981-82 period and it was validated on the rest of the available data as shown in Table 1.

Table 1. Performance criteria of the SACRAMENTO model

Period	*EV*	*EFF*
1980-82	0.750	0.749
1977-80	0.733	0.733
1982-86	0.705	0.705
1977-86	0.728	0.728

Comparison plots of the estimated and measured daily discharges for 1-month periods are shown in Figures 3, 4 and 5.

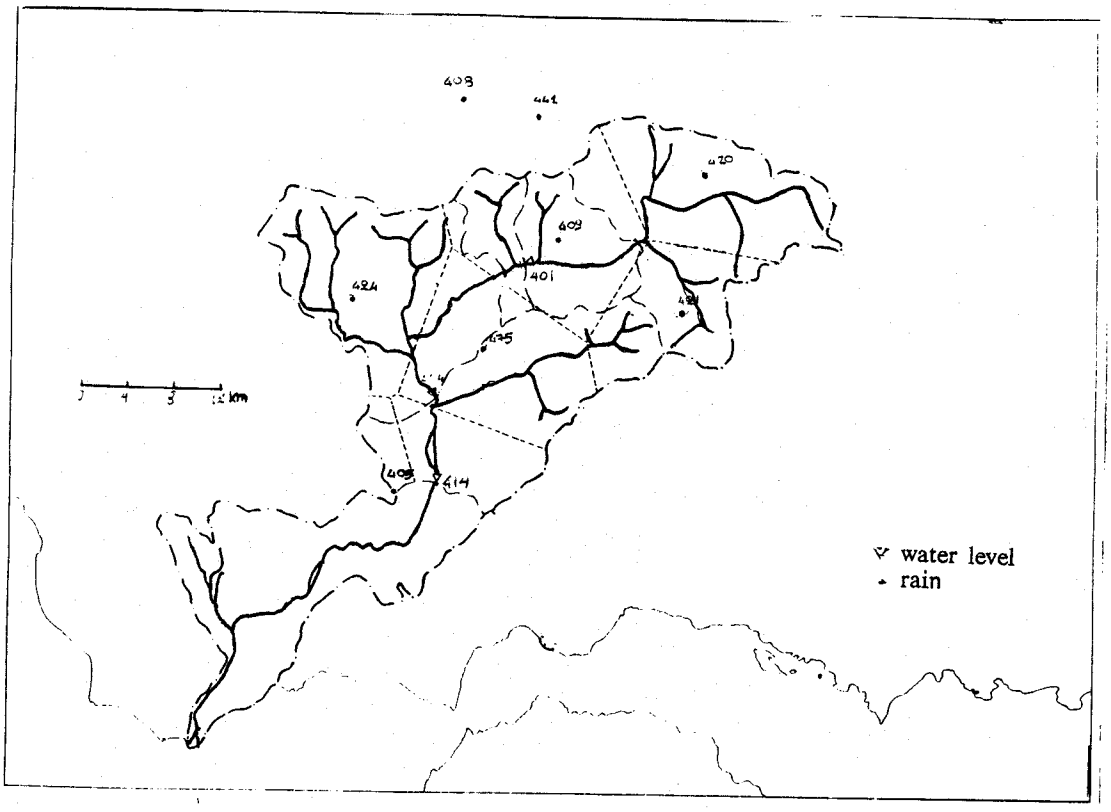

Fig. 2 The Evinos River Basin

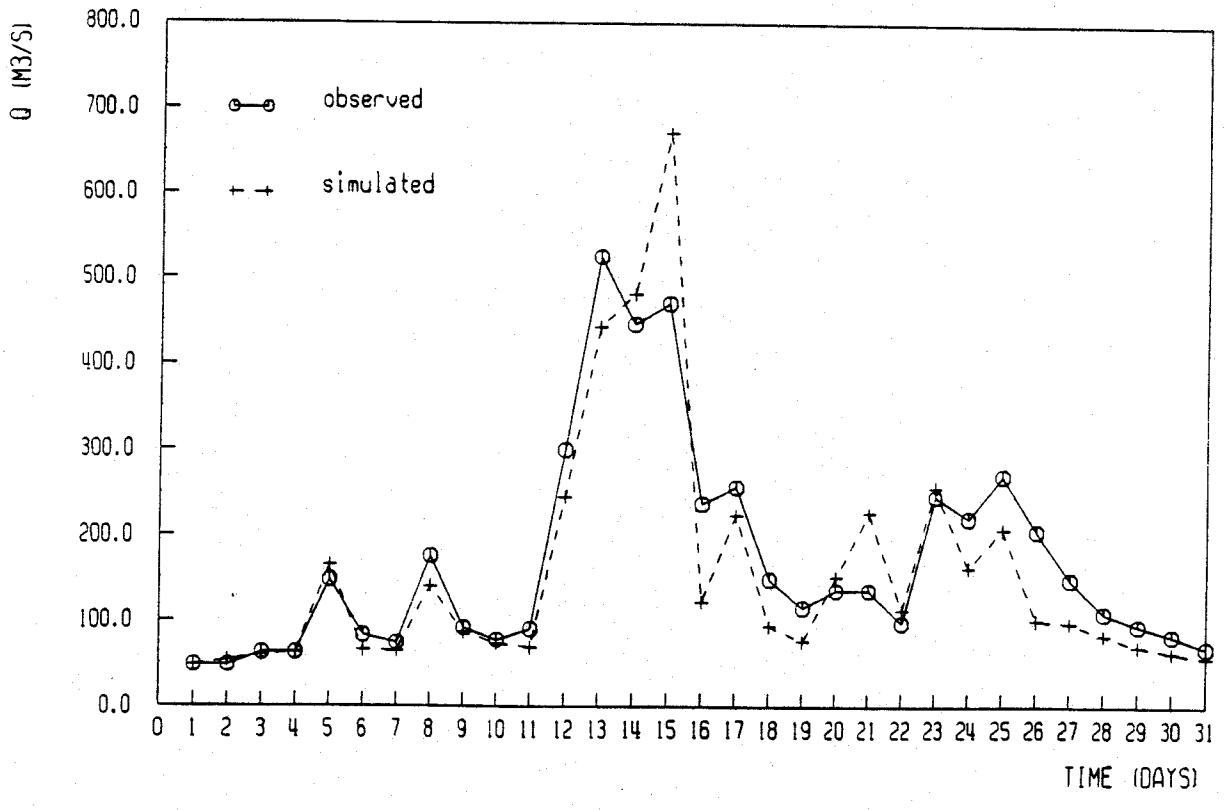

Fig. 3 Comparison of estimated and measured discharge-December 1981-Calibration period

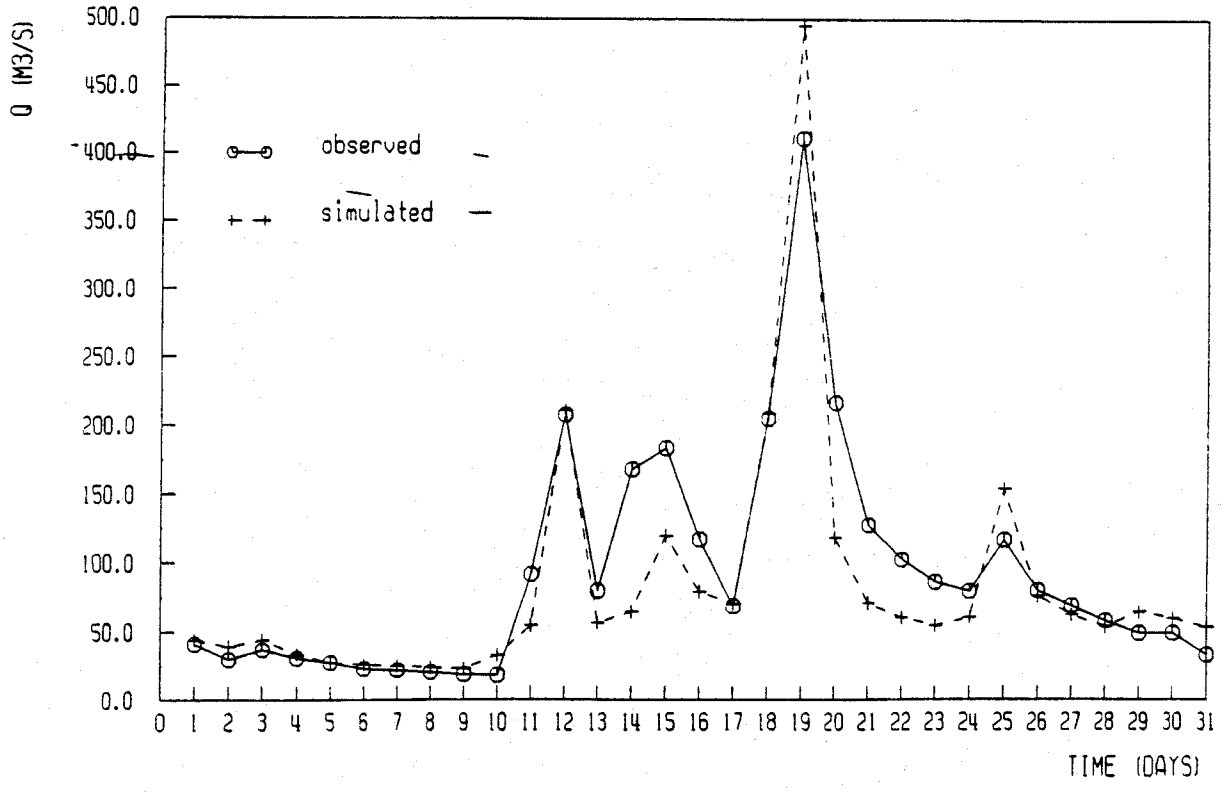

Fig. 4 Comparison of estimated and measured discharge-December 1982-Verification period

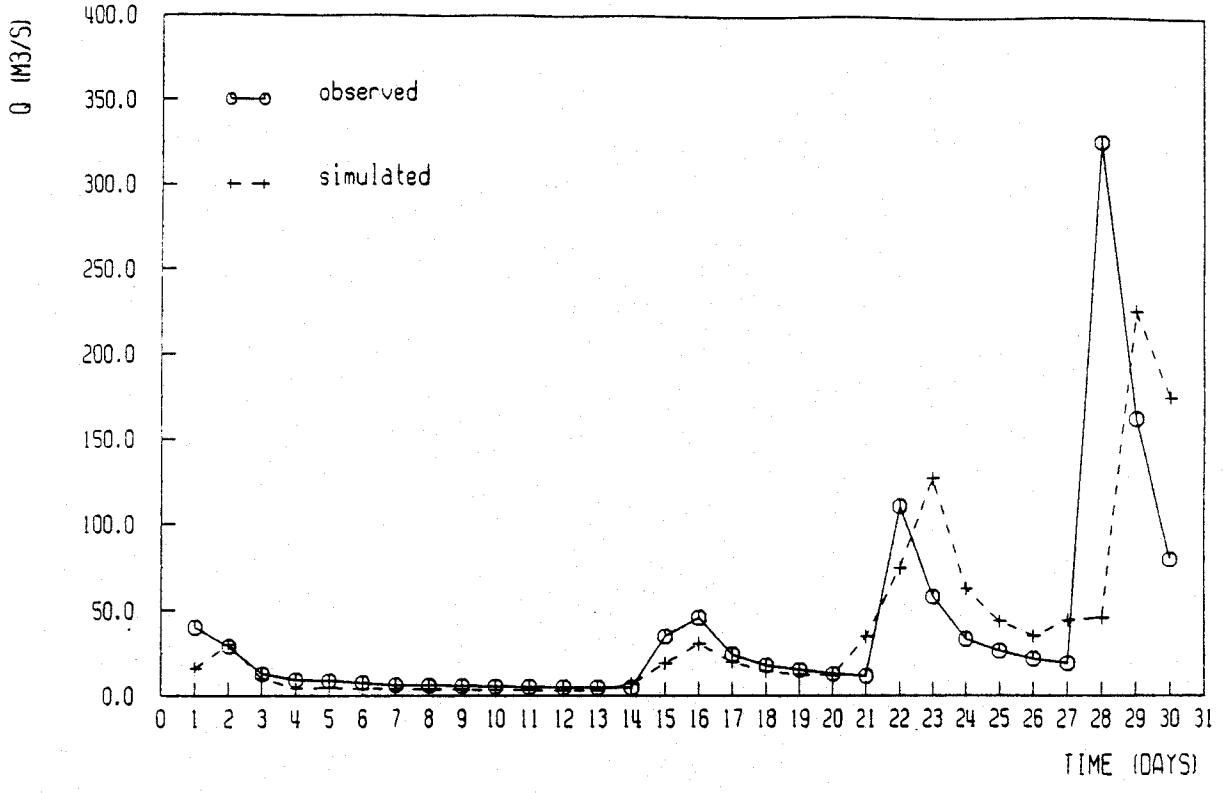

Fig. 5 Comparison of estimated and measured discharge-November 1983-Verification period

4. FUTURE RESEARCH

Testing of the SACRAMENTO model within the framework proposed in section 1 will be completed. The hourly version of the model will be calibrated based on a continuous-time data set of the Evinos River Basin at Poros Righaniou. The calibration will involve the following steps:

1. Calibration of the Transfer Function or Unit Hydrograph independently of the runoff production model. The calibration will be performed by the FDTF method (Guillot and Duband, 1980, Nalbantis, 1987, Nalbantis et al., 1988, Rodriguez et al., 1988, Duband et al., 1990).
2. Calibration of the SACRAMENTO model as a runoff production submodel using the already identified Unit Hydrograph.
3. Validation of the hourly model.
4. Testing the possibility of incorporating within the hourly model extra information coming from the daily model.
5. Extension of the analysis to another model e.g. XINANJIANG (Franchini and Pacciani, 1989, 1991).
6. Application to the Reno River Basin, Italy and possibly another European catchment.

The steps 2 to 6 are expected to be completed during the second year of the project.

REFERENCES

Burnash, R. J. C., R. L. Ferral, and R. A. McGuire, *A generalized streamflow simulation system-conceptual modeling for digital computers*, Joint Federal State River Forecasting Center, Sacramento, Calif., 1973.

Duband D., I. Nalbantis, C. Obled, J. Y. Rodriguez and P. Tourasse, Unit Hydrograph revisited through differencing and deconvolution on multi-event data sets: the FDTF approach, *IAHS publ., 190*, 377-390, 1990

Franchini, M. and M. Pacciani, *Analisi comparativa di alcuni modelli afflusi deflussi di tipo concettuale*, University of Bologna, Bologna, 1989

Franchini, M. and M. Pacciani, Comparative analysis of several conceptual rainfall-runoff models, *J. Hydrol., 122*, 161-219, 1991

Guillot P. and D. Duband, Fonctions de transfert pluie-debit sur des bassins versants de l'ordre de 1000 km^2, *IAHS publ., 129*, 177-186, 1980

Gupta V. K. and S. Sorooshian, Uniqueness and observability of conceptual rainfall-runoff model parameters. The percolation process examined, *Water Resour. Res., 17*(1), 269-276, 1981

Gupta V. K. and S. Sorooshian, The automatic calibration of conceptual rainfall-runoff models using derivative-based optimization algorithms, *Water Resour. Res., 21*(4), 473-485, 1985

Nalbantis I., *Identification de modeles pluie-debit du type Hydrogramme Unitaire: Developpements de la methode DPFT et validation sur donnees simulees avec et sans erreur*, Ph. D. thesis, Grenoble, 1987

Nalbantis I., C. Obled and J. Y. Rodriguez, Modelisation pluie-debit: validation par simulation de la methode DPFT, *La Houille Blanche, 5/6*, 415-424, 1988

Rodriguez J. Y., I. Nalbantis and C. Obled, Rainfall-runoff modeling by the FDTF method. Testing and validation by generated data, *Proc. 4th int. Symp. on Systems Analysis applied to Management of Water Resources*, Rabat, Morocco.

Sorooshian S., V. K. Gupta and J. L. Fulton, Evaluation of maximum likelihood parameter estimation techniques for conceptual rainfall-runoff models, *Water Resour. Res., 19*(1), 251-259, 1983a

Sorooshian S. and V. K. Gupta, Automatic calibration of conceptual rainfall-runoff models: The question of parameter observability and uniqueness, *Water Resour. Res., 19*(1), 260-268, 1983b

Sorooshian S. and V. K. Gupta, The analysis of structural identifiability: Theory and application to conceptual rainfall-runoff models, *Water Resour. Res., 21*(4), 487-495, 1985

COMMISSION OF EUROPEAN COMMUNITIES

NATIONAL TECHNICAL UNIVERSITY OF ATHENS
DIVISION OF WATER RESOURCES - HYDRAULIC AND MARITIME ENGINEERING

A F O R I S M:
A COMPREHENSIVE FORECASTING SYSTEM FOR FLOOD RISK MITIGATION AND CONTROL

ANNEX 3

RAINFALL-RUNOFF MODELING IN A MEDITERRANEAN ENVIRONMENT: UNIT HYDROGRAPH ESTIMATION THROUGH THE FDTF METHOD

by: I. Nalbantis

CONTRACT NO.: EPOC-CT90-0023
PROJECT COORDINATOR: PROF. E. TODINI
GROUP LEADER: PROF. TH. S. XANTHOPOULOS

ATHENS - JUNE 1992

Rainfall-Runoff Modeling in a Mediterranean Environment: Unit Hydrograph estimation through the FDTF method

by Ioannis Nalbantis

National Technical University of Athens

Division of Water Resources, Hydraulic and Maritime Engineering,

5 Iroon Polytechniou 15700 Zografou, Greece

CONTENTS

1. INTRODUCTION

It is known that rainfall-runoff models that are parts of modern flood forecasting systems, require high quality and adequate quantity of data. In the first report of the AFORISM project in February 1992 the data paucity in southern European countries was stressed and a framework for model testing was proposed. The scarcity of recording devices causes problems to the model calibration at least in the early stages of the establishment of a flood forecasting system. In such a situation the calibration must be based on a very short record coming from a newly built data collection system, and it must ignore the old data that seem to be inadequate. The problem posed is to examine the possibility of extracting information from daily data in order to use it within a short time-step (e.g. hourly) rainfall-runoff model.

Suppose that we need hourly data for our rainfall-runoff model. The following framework for model testing has been proposed in the First Report on AFORISM project (1992):

1. Calibration of an hourly rainfall-runoff model on a short continuous-time data record (record 1).
2. Verification of the same hourly rainfall-runoff model on a short continuous-time data record (record 2).
3. Calibration of a daily rainfall-runoff model, having the same structure with the hourly model based on a relatively long continuous-time data record (record 3).
4. Verification of the above daily rainfall-runoff model on a relatively long continuous-time data record (record 4).
5. Use of some parameters of the daily model either directly or after transformation within the hourly model and verification the latter model based on record 2.
6. Comparison of the results
7. Extension to other models.

The SACRAMENTO model (Burnash et al., 1973) was chosen to be the first model to test. This model was calibrated and validated on daily data of the Evinos River Basin. Steps 3 and 4 in our framework for model testing, were followed. Note that steps 3 and 4 are independent from steps 1 and 2. Therefore, the order of application of these two groups of steps is unimportant. In this report we present our work on the identification of a short time step (hourly) model. The overall model is decomposed into two submodels:

- A soil moisture accounting submodel or Production Function

- A Transfer Function of the runoff volume produced by the previous model to the outlet.

The SACRAMENTO model or any other model that will be tested will play the role of a Production Function, whereas for the transfer function part, a Linear Transfer Function or Unit Hydrograph will be used for all Production Functions. It follows that the initial transfer function in all models will not be activated. In this report we present our work on the Transfer Function identification within step 1 of the above framework. The First Differenced Transfer Function (or FDTF) method was used. In the following sections we first describe the principles of the method and then we present the results and the future research proposed.

2. DESCRIPTION OF THE FDTF METHOD

The FDTF approach initially proposed by Duband (1978) and Guillot and Duband (1980) is an extension of the classical Unit Hydrograph method. It assumes that the areal precipitation over the basin is transformed into runoff at the outlet following the two processes:

- A Runoff Production Function which yields a value of excess rainfall for every time step. This function is generally highly non-linear.
- A linear Transfer Function which transfers the excess rainfall volumes to the outlet of the basin.

Additionally, the method operates in a multi-event context. Suppose that we have N events with n_j (j = 1,2,3,...,N) time steps each. We define as $R_{i,j}$ the measured areal rainfall for the i-th time step of the j-th event. Similarly we define $P_{i,j}$ and $Q_{i,j}$ the excess rainfall and measured discharge for the i-th time step of the j-th event. The Transfer Function is expressed as a convolution equation:

$$Q_{i,j} = \sum_{k=1}^{K} H_k \, P_{i-k+1,j} + \varepsilon_{i,j} \qquad (1)$$

where

K is the memory length of the Transfer Function,

H_k is the k-th ordinate of the Transfer Function (k = 1,2,3,...,K). and

$\varepsilon_{i,j}$ is the model's error for the i-th time step of the j-th event.

The method identifies two sets of unknowns: The excess rainfall $P_{i,j}$ for each time step i and each event j as well as a Transfer Function with ordinates H_k for a finite memory length K, common to all events. The identification problem which is non-linear, is solved iteratively by the FDTF algorithm which is similar to the Gradient algorithm (Versiani, 1983) and it is schematized as follows:

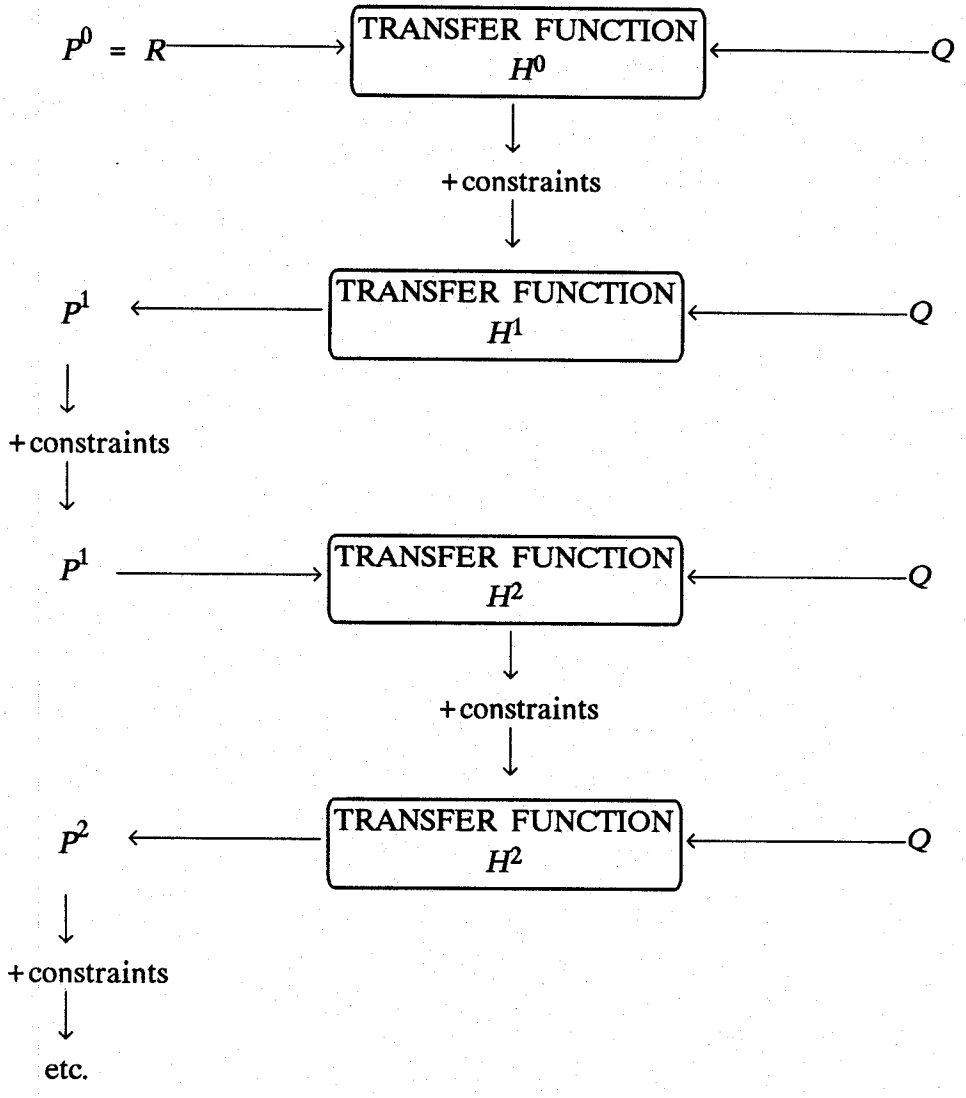

Figure 1. The FDTF algorithm-First 2 iterations

A first guess for excess rainfall P^0 is considered to be the measured rainfall R. A first estimate H^1 for the ordinates of the Transfer Function is obtained based on P^0 and the measured discharge Q. Then some feasibility constraints are imposed on the coefficients of the Transfer Function. A deconvolution is performed to give a better estimate P^1 for the

excess rainfall series based on these coefficients and the series of observed discharges Q. Here constraints are also applied and a new iteration begins. Based on P^1 and Q, an improved estimate of the Transfer Function is obtained and so on.

The method operates on the first differences of the observed discharges $q_{i,j} = Q_{i,j} - Q_{i-1,j}$ for the following reasons: (i) the coefficients of the FDTF are more decorrelated than those of the Transfer Function, (ii) differencing filters the baseflow; thus, arbitrary baseflow separation is by-passed and (iii) the quantity that is really sought in a flood forecasting situation is the first difference of the discharge and not the discharge itself. From equation 1 it follows

$$q_{i,j} = \sum_{k=1}^{K} h_k \, P_{i-k+1,j} + \varepsilon_{i,j} \qquad (2)$$

with the First Differenced Transfer Function or FDTF derived from the Transfer Function as

$$h_1 = H_1$$
$$h_k = H_k - H_{k-1}$$
$$h_{k+1} = -H_{k+1} = 0$$

Once the FDTF has been computed the Transfer Function is easily obtained by a simple summation. The constraints applied on the ordinates of the Transfer Function are

- Non-negativity constraint; that is if $H_k<0$ then we set $H_k=0$
- Mass conservation law expressed as $\sum_{k=1}^{K} H_k = 1$. In practice we force this sum to be 1. .

The constraints imposed on excess rainfalls after the deconvolution phase has ended, are the following:

- Non-negativity constraint; that is if $P_{i,j}<0$ then we set $P_{i,j}=0$
- Mass conservation law implies that $P_{i,j} \leq R_{i,j}$ but $R_{i,j}$ are rarely known with sufficient accuracy to justify such a constraint.

We can write equation 2 for any event j with duration n_j time steps. By omitting subscript j and the error term we obtain the following system of equations

$$\begin{pmatrix} q_1 \\ q_2 \\ q_3 \\ q_4 \\ \cdot \\ \cdot \\ q_{k-1} \\ q_k \\ q_{k+1} \\ \cdot \\ \cdot \\ q_{m-1} \\ q_m \\ q_{m+1} \\ q_{m+2} \\ \cdot \\ \cdot \\ q_{n-2} \\ q_{n-1} \\ q_n \end{pmatrix} = \begin{pmatrix} P_1 & 0 & 0 & 0 & 0 & . & . & 0 & 0 \\ P_2 & P_1 & 0 & 0 & 0 & . & . & 0 & 0 \\ P_3 & P_2 & P_1 & 0 & 0 & . & . & 0 & 0 \\ P_4 & P_3 & P_2 & P_1 & 0 & . & . & 0 & 0 \\ \cdot & \cdot & \cdot & \cdot & \cdot & . & . & \cdot & \cdot \\ \cdot & \cdot & \cdot & \cdot & \cdot & . & . & \cdot & \cdot \\ P_{k-1} & P_{k-2} & P_{k-3} & P_{k-4} & P_{k-5} & . & . & P_1 & 0 \\ P_k & P_{k-1} & P_{k-2} & P_{k-3} & P_{k-4} & . & . & P_2 & P_1 \\ P_{k+1} & P_k & P_{k-1} & P_{k-2} & P_{k-3} & . & . & P_3 & P_2 \\ \cdot & \cdot & \cdot & \cdot & \cdot & . & . & \cdot & \cdot \\ \cdot & \cdot & \cdot & \cdot & \cdot & . & . & \cdot & \cdot \\ P_{m-1} & P_{m-2} & P_{m-3} & P_{m-4} & P_{m-5} & . & . & P_{m-K+1} & P_{m-K} \\ P_m & P_{m-1} & P_{m-2} & P_{m-3} & P_{m-4} & . & . & P_{m-K+2} & P_{m-K+1} \\ 0 & P_m & P_{m-1} & P_{m-2} & P_{m-3} & . & . & P_{m-K+3} & P_{m-K+2} \\ 0 & 0 & P_m & P_{m-1} & P_{m-2} & . & . & P_{m-K+4} & P_{m-K+3} \\ \cdot & \cdot & \cdot & \cdot & \cdot & . & . & \cdot & \cdot \\ \cdot & \cdot & \cdot & \cdot & \cdot & . & . & \cdot & \cdot \\ 0 & 0 & 0 & 0 & 0 & . & . & P_{m-1} & P_{m-2} \\ 0 & 0 & 0 & 0 & 0 & . & . & P_m & P_{m-1} \\ 0 & 0 & 0 & 0 & 0 & . & . & 0 & P_m \end{pmatrix} \times \begin{pmatrix} h_1 \\ h_2 \\ h_3 \\ h_4 \\ \cdot \\ \cdot \\ h_{K-1} \\ h_K \end{pmatrix}$$

Writing the same system in a matrix form as $\mathbf{q}_j = \mathbf{P}_j\mathbf{h}$ we obtain for a set of N events

$$\begin{pmatrix} \mathbf{q}_1 \\ \mathbf{q}_2 \\ \mathbf{q}_3 \\ \cdot \\ \mathbf{q}_{j-1} \\ \mathbf{q}_j \\ \mathbf{q}_{j+1} \\ \cdot \\ \mathbf{q}_{N-1} \\ \mathbf{q}_N \end{pmatrix} = \begin{pmatrix} \mathbf{P}_1 \\ \mathbf{P}_2 \\ \mathbf{P}_3 \\ \cdot \\ \mathbf{P}_{j-1} \\ \mathbf{P}_j \\ \mathbf{P}_{j+1} \\ \cdot \\ \mathbf{P}_{N-1} \\ \mathbf{P}_N \end{pmatrix} \times \mathbf{h}$$

This system is overdetermined and it can be solved, for example by ordinary least squares.

In the deconvolution phase we can write for the j-th event after omission of subscripts j

$$\begin{pmatrix} q_1 \\ q_2 \\ q_3 \\ q_4 \\ . \\ . \\ q_{k-1} \\ q_k \\ q_{k+1} \\ . \\ . \\ q_{m-1} \\ q_m \\ q_{m+1} \\ . \\ . \\ q_{n-2} \\ q_{n-1} \\ q_n \end{pmatrix} = \begin{pmatrix} h_1 & 0 & 0 & 0 & . & 0 & 0 & . & 0 \\ h_2 & h_1 & 0 & 0 & . & 0 & 0 & . & 0 \\ h_3 & h_2 & h_1 & 0 & . & 0 & 0 & . & 0 \\ h_4 & h_3 & h_2 & h_1 & . & 0 & 0 & . & 0 \\ . & . & . & . & . & . & . & . & . \\ . & . & . & . & . & . & . & . & . \\ h_{k-1} & h_{k-2} & h_{k-3} & h_{k-4} & . & h_1 & 0 & . & 0 \\ h_k & h_{k-1} & h_{k-2} & h_{k-3} & . & h_2 & h_1 & . & 0 \\ h_{k+1} & h_k & h_{k-1} & h_{k-2} & . & h_3 & h_2 & . & 0 \\ . & . & . & . & . & . & . & . & . \\ . & . & . & . & . & . & . & . & . \\ h_{m-1} & h_{m-2} & h_{m-3} & h_{m-4} & . & h_{m-K+1} & h_{m-K} & . & 0 \\ h_m & h_{m-1} & h_{m-2} & h_{m-3} & . & h_{m-K+2} & h_{m-K+1} & . & h_1 \\ h_{m+1} & h_m & h_{m-1} & h_{m-2} & . & h_{m-K+3} & h_{m-K+2} & . & h_2 \\ & & & & . & & & . & \\ & & & & . & & & . & \\ h_{n-2} & h_{n-3} & h_{n-4} & h_{n-5} & . & h_{n-K} & h_{n-K-1} & . & h_{K-2} \\ h_{n-1} & h_{n-2} & h_{n-3} & h_{n-4} & . & h_{n-K+1} & h_{n-K} & . & h_{K-1} \\ h_n & h_{n-1} & h_{n-2} & h_{n-3} & . & h_{n-K+2} & h_{n-K+1} & . & h_K \end{pmatrix} \times \begin{pmatrix} P_1 \\ P_2 \\ P_3 \\ P_4 \\ . \\ P_{K-1} \\ P_K \\ . \\ P_m \end{pmatrix}$$

Note that the coefficients h_k with k greater than the memory length K are not identified but they are estimated by extrapolating the Transfer Function with an exponential curve.

The above system of equations can be written in the matrix form $\mathbf{q}_j = \mathbf{H}_j\mathbf{p}_j$ is overdetermined. It can be solved by ordinary least squares but we face frequent problems of instability due to the correlation of h's.

A number of variants of the method were developed (Versiani, 1983; Nalbantis, 1987, Nalbantis et al., 1988, Rodriguez et al., 1988, Rodriguez, 1989, Duband et al., 1990) The variants which have been thoroughly tested by Nalbantis (1987) are the following:

- Transfer Function identification
  - Ordinary Least Squares
  - ARMAX models
  - Constrained Least Squares
- Deconvolution
  - = Ordinary least squares
  - Ridge regression
  - Linear programming

The method has been tested on synthetic data (Nalbantis, 1987). Guidelines for users are given by Nalbantis (1987) and summarized by Sempere Torres (1990).

3. RESULTS

We applied the FDTF method to identify the Transfer Function or the Unit Hydrograph of the Evinos River Basin at Poros Righaniou (see Fig. 1). The area of the basin is 884 km^2 and the average ground elevation is +990 m. Hourly data for 20 flood events within the period 1973-1988 were used. Rainfall data from 3 recording rain gauges were collected, digitized and processed. These stations together with by their codes shown in Figure 1, are: Drymonas(424), Krikelo(441) and Aniada(408). The rating curves were derived from the hydrometric data. The Transfer Function identified is depicted in Figure 2. The overall Determination Coefficient R^2 varied from 0.823 in the first iteration to 0.918 in the last (fifth) iteration. As to the individual events, R^2 varied from 0.723 to 0.980 in the last iteration. For the vast majority of events R^2 was greater than 0.90. In Figures 3 and 4 we compare the measured and the calculated hydrographs for 2 events with high peak discharge values.

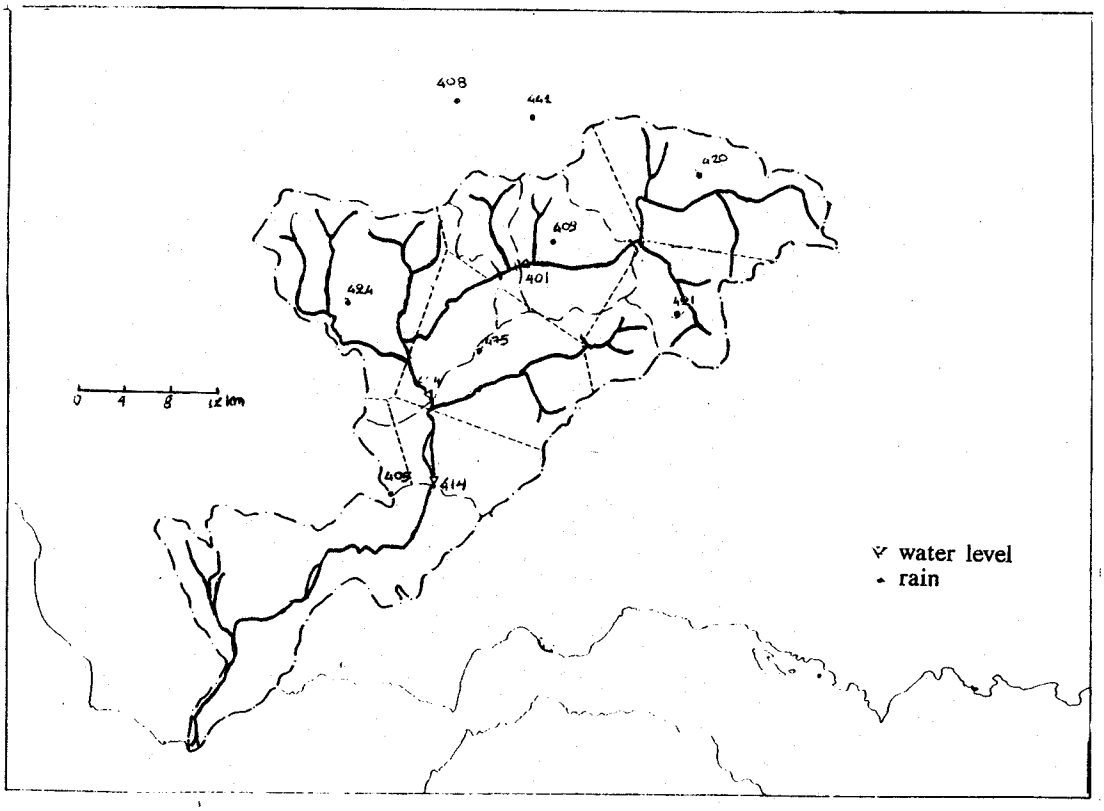

Fig. 1 The Evinos River Basin

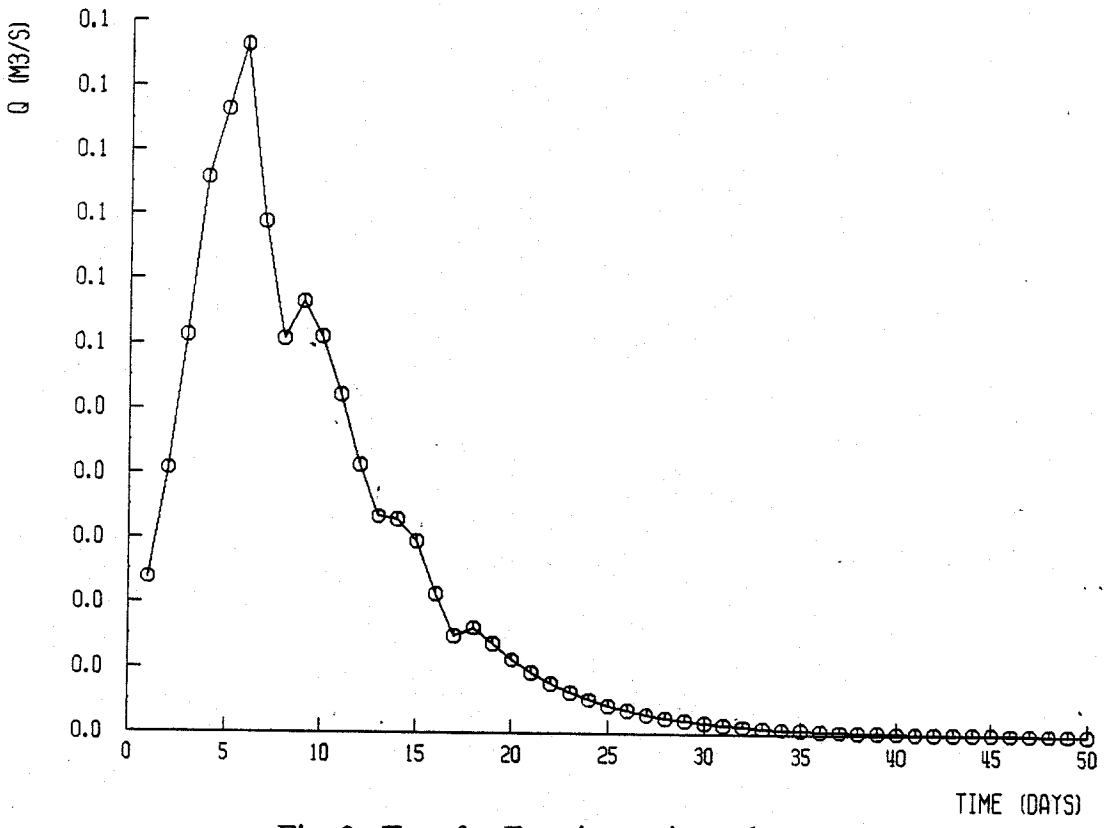

Fig. 2 Transfer Function estimated

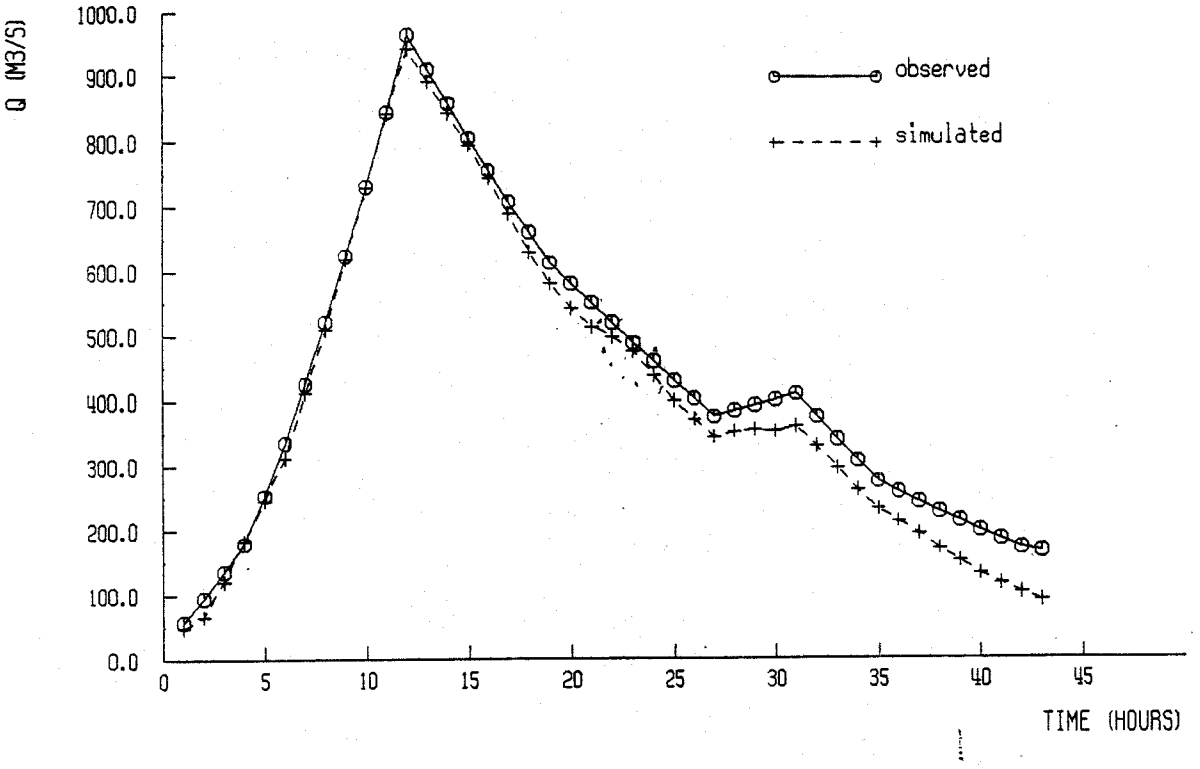

Fig. 3 Comparison of estimated and measured discharge-Calibration period

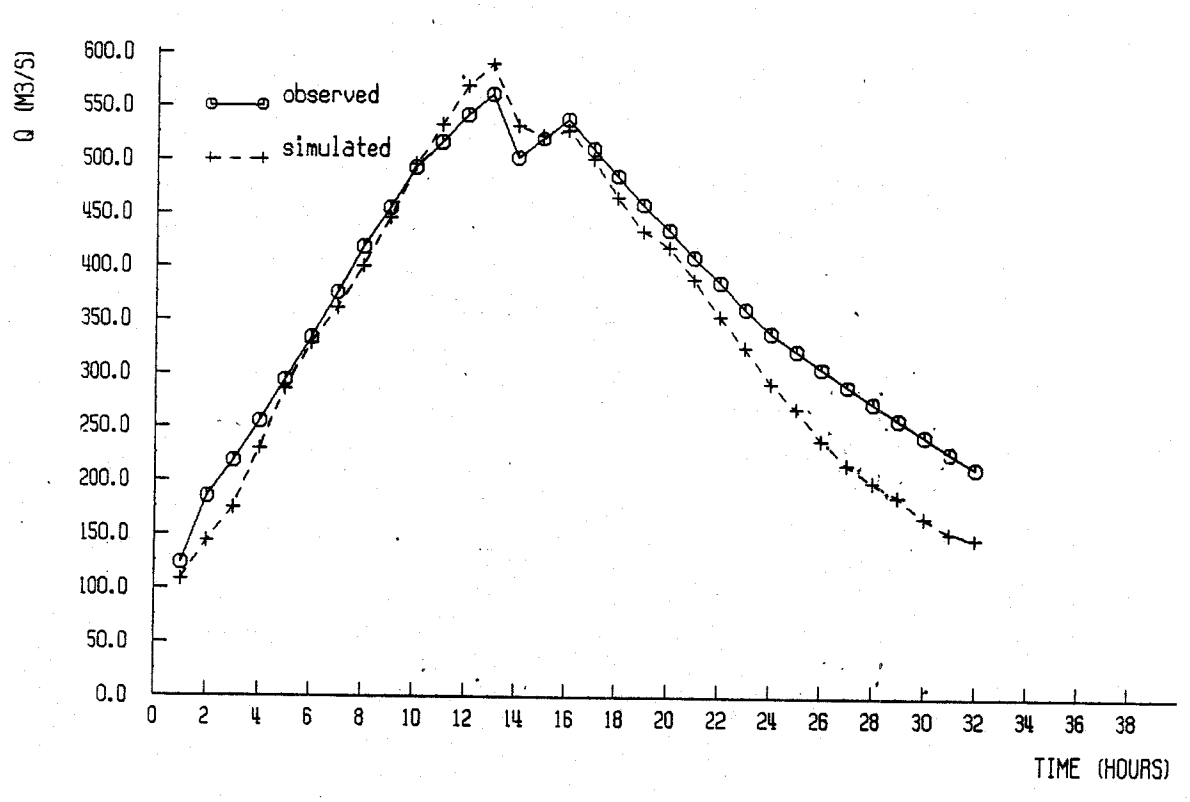

Fig. 4 Comparison of estimated and measured discharge-Calibration period

4. FUTURE RESEARCH

The SACRAMENTO model testing will be completed within the framework proposed in section 1. The hourly version of the model will be calibrated on a continuous-time data set of the Evinos River Basin at Poros Righaniou. The calibration will involve the following steps:

1. Calibration of the SACRAMENTO model as a runoff production submodel using the already identified Unit Hydrograph.
2. Validation of the hourly model.
3. Testing the possibility of incorporating within the hourly model, extra information coming from the daily model
4. Extension of the analysis to another model e.g. XINANJIANG (Franchini and Pacciani, 1989, 1991).
6. Application to the Reno River Basin, Italy and possibly another European catchment.

The steps 2 to 6 are expected to be completed during the second year of the project.

REFERENCES

Burnash, R. J. C., R. L. Ferral, and R. A. McGuire, *A generalized streamflow simulation system-conceptual modeling for digital computers*, Joint Federal State River forecasting Center, Sacramento, Calif., 1973.

Duband D. Internal report, EDF-DTG, Grenoble, 1978

Duband D., I. Nalbantis, c. Obled, J. Y. Rodriguez and P. Tourasse, Unit Hydrograph revisited through differencing and deconvolution on multi-event data sets: the FDTF approach, *IAHS publ., 190*, 377-390, 1990

Franchini, M. and M. Pacciani, *Analisi comparativa di alcuni modelli afflusi deflussi di tipo concettuale*, University of Bologna, Bologna, 1989

Franchini, M. and M. Pacciani, Comparative analysis of several conceptual rainfall-runoff models, *J. Hydrol., 122*, 161-219, 1991

Guillot P. and D. Duband, Fonctions de transfert pluie-debit sur des bassins versants de l'ordre de 1000 km^2, *IAHS publ., 129*, 177-186, 1980

Nalbantis I., *Identification de modeles pluie-debit du type Hydrogramme Unitaire: Developpements de la methode DPFT et validation sur donnees simulees avec et sans*

erreur, Ph. D. thesis, Grenoble, 1987

Nalbantis I., C. Obled and J. Y. Rodriguez, Modelisation pluie-debit: validation par simulation de la methode DPFT, *La Houille Blanche, 5/6*, 415-424, 1988

Rodriguez J. Y., I. Nalbantis and C. Obled, Rainfall-runoff modeling by the FDTF method. Testing and validation by generated data, *Proc. 4th int. Symp. on Systems Analysis applied to Management of Water Resources*, Rabat, Morocco, 1988.

Rodriguez J. Y., *Modelisation pluie-debit par la methode DPFT: developpements de la methode initiale et extension a des cas bi-entrees*, Ph. D. thesis, INPG, Grenoble, 1989

Sempere Torres D., *Calcul de la lame ruissellee dans la modelistion pluie-debit: Limitations des approches globales et introduction simplifiee dse la topographie et de la variabilite spatiale des pluies*, Ph. D. thesis, INPG, Grenoble, 1990

Versiani B., Modelisation de la relation pluie-debit pour la prevision de crues, Ph,\. D. thesis, INPG, Grenoble, 1983

COMMISSION OF EUROPEAN COMMUNITIES

NATIONAL TECHNICAL UNIVERSITY OF ATHENS
DIVISION OF WATER RESOURCES - HYDRAULIC AND MARITIME ENGINEERING

A F O R I S M:
A COMPREHENSIVE FORECASTING SYSTEM FOR FLOOD RISK MITIGATION AND CONTROL

ANNEX 4

A STUDY OF THE TEMPORAL STRUCTURE OF STORMS BY USING SCALING MODELS

by: D. Koutsoyiannis & E. Foufoula

CONTRACT NO.: EPOC-CT90-0023
PROJECT COORDINATOR: PROF. E. TODINI
GROUP LEADER: PROF. TH. S. XANTHOPOULOS

ATHENS - JUNE 1992

A study of the temporal structure of storms by using scaling models

Demetris Koutsoyiannis and Efi Foufoula

Contents

ABSTRACT

Empirical evidence suggests that statistical properties of storm rainfall at a location and within a homogeneous season have a well structured dependence on storm duration. For example, the mean and standard deviation of total storm depth increase with duration each according to a power law with the same exponent; the lag-one correlation coefficient of hourly rainfall depths increases with duration; and the decay rate of the autocorrelation function of hourly rainfall depths decreases with duration. Motivated by the first observation, a simple scaling model for rainfall intensity within a storm was hypothesized and was shown both analytically and empirically that such a model can explain reasonably well the observed statistical structure in the interior of storms providing thus an efficient parametrization of storms of varying durations and total depths. This simple scaling model is also consistent with, and provides a theoretical basis for, the concept of mass curves (normalized cumulative storm depth vs. normalized cumulative time since the beginning of a storm) which are extensively used in hydrologic design. In contrast, popular stationary models of rainfall intensity are shown unable to capture the duration dependent statistical structure of storm depths and are also inconsistent with the concept of mass curves.

1 Introduction

This study deals with the analysis and modeling of the stochastic structure of rainfall intensities within storms of varying duration. Storms are defined here as rainfall events which are independent of each other as based, for example, on Poisson storm arrivals. The need to parametrize the time distribution of storms which are "similar" apart from total storm depth and storm duration arose very early and the concept of mass curves, i.e., non-dimensional cumulative storm depth versus non-dimensional cumulative time since the beginning of a storm, has been extensively used for hydrologic design (e.g., Huff, 1967; Pilgrim and Cordery, 1975; among others). The idea behind those efforts was the recognition that for a particular location or within a meteorologically homogeneous region and for a homogeneous season, storms are expected to exhibit similarities in their internal structure despite their different durations and total storm depths.

In this study, we provide empirical evidence that the statistical properties of incremental storm depths, e.g., hourly depths, and total storm depths have a well structured dependence on storm duration. For example, it is found that the mean and standard deviation of the total storm depth increase with duration each according to a power law with the same exponent, i.e., the coefficient of variation of total storm depth is independent of storm duration (see, for example, Fig. 4 to be discussed in detail later). This motivates the hypothesis of a simple scaling model for the instantaneous rainfall intensity within a storm with storm duration as the scaling parameter. This model has been thoroughly examined in this study and the properties of the total storm depth and incremental rainfall depths have been analytically derived and have been used for model fitting and model evaluation. Another motivation for examining the simple scaling model is that it is consistent with the concept of mass curves which are very often used in hydrologic applications.

Most of the available continuous time rainfall models, e.g., the Neyman-Scott rectangular pulses model (Rodriguez-Iturbe et al., 1984) used to describe rainfall intensities are stationary. In this study we show that any stationary model is unable to capture the duration dependent statistical structure of rainfall intensities and is also inconsistent with the concept of mass curves.

This study is structured as follows. Section 2 introduces notation. In section 3 the simple scaling model for instantaneous rainfall intensities within a storm is presented. The statistical properties of the total storm depth and incremental storm depths, e.g., hourly depths, are derived in section 4. In section 5 the simple scaling model is fitted to hourly data from 89 storms in Chalara, Greece and the performance of the model is evaluated in terms of its ability to capture statistical properties not explicitly used for model fitting. In section 6 two stationary models of instantaneous rainfall intensity are examined and it is shown both analytically and empirically that these models are

not able to reproduce some of the observed characteristics of storm rainfall that the simple scaling model is able to describe. In section 7 the connection of simple scaling models to mass curves is examined and it is shown that mass curves are consistent with the hypothesis of simple scaling but are inconsistent with the assumption of any stationary model for instantaneous rainfall intensities.

2 Terminology and preliminaries

Let D denote the duration of a storm and $\xi(t, D)$, $0 \leq t \leq D$ the rainfall intensity process within the storm duration. $h(t, D)$ denotes the cumulative rainfall depth process defined as

$$h(t, D) = \int_0^t \xi(s, D) ds, \quad 0 \leq t \leq D \tag{1}$$

and $h^*(t, D) = h(t, D)/h(D, D)$ the nondimensionalized rainfall depth process (see Fig. 1). Let $X_\Delta(i, D)$ denote the incremental rainfall depth in the interval $((i-1)\Delta, i\Delta)$ i.e.,

$$X_\Delta(i, D) = \int_{(i-1)\Delta}^{i\Delta} \xi(t, D) dt, \quad i = 1, 2, ...k \tag{2}$$

where k is the integer part of D/Δ. It is assumed that within a meteorologically homogeneous region and season every storm of duration D can be considered as a realization of an ensemble characterized by that duration.

Let $\eta_\xi(t, D)$ denote the ensemble average of $\xi(t, D)$, i.e.,

$$\eta_\xi(t, D) = E[\xi(t, D)] \tag{3}$$

and $R_\xi(t_1, t_2; D)$ the second order product moment of $\xi(t, D)$ in the interval of a storm event, i.e.,

$$R_\xi(t_1, t_2; D) = E[\xi(t_1, D)\xi(t_2, D)], \quad 0 \leq t_1, t_2 \leq D \tag{4}$$

where again expectation refers to ensemble average. The covariance function of $\xi(t, D)$ is then given as

$$C_\xi(t_1, t_2; D) = Cov[\xi(t_1, D)\xi(t_2, D)] = R_\xi(t_1, t_2; D) - \eta_\xi(t_1, D)\eta_\xi(t_2, D) \tag{5}$$

In a similar manner we define the statistical properties of the cumulative depth process $h(t, D)$, i.e., $\eta_h(t, D)$, $R_h(t_1, t_2; D)$, and $C_h(t_1, t_2; D)$, and those of the incremental depth process $X_\Delta(t, D)$, i.e., $\eta_{X_\Delta}(i, D)$, $R_{X_\Delta}(i, j; D)$, and $C_{X_\Delta}(i, j; D)$.

3 Simple scaling model for storm intensities

The hypothesis is set forward that the process of instantaneous rainfall intensities within a storm, i.e., $\xi(t,D)$, $0 \le t \le D$ is a self-similar (simple scaling) process with scaling exponent H, i.e.,

$$\{\xi(t,D)\} \stackrel{d}{=} \{\lambda^{-H}\xi(\lambda t, \lambda D)\} \tag{6}$$

where the above equality is in terms of the finite dimensional probability distribution, i.e.,

$$Pr[\xi(t_1,D) \le x_1,\ldots,\xi(t_n,D) \le x_n] = Pr[\lambda^{-H}\xi(\lambda t_1,\lambda D) \le x_1,\ldots,\lambda^{-H}\xi(\lambda t_n,\lambda D) \le x_n], \quad 0 \le t_1,\ldots,t_n \le D \tag{7}$$

(see, for example, Lamperti 1962, where, however, infinite duration stochastic processes are considered). Consequently the k-th moment of $\xi(t,D)$ is given as

$$E[\xi(t,D)^k] = \lambda^{-Hk}E[\xi(\lambda t,\lambda D)^k] \tag{8}$$

and the (k,l) second product moment as

$$E[\xi(t_1,D)^k\xi(t_2,D)^l] = \lambda^{-H(k+l)}E[\xi(\lambda t_1,\lambda D)^k\xi(\lambda t_2,\lambda D)^l] \tag{9}$$

An intuitive feeling of the notion of scaling in (6) can be obtained from Figure 2 where, for example, if $D_2 = \lambda D_1$ then under appropriate scaling of time, i.e., $t_2 = \lambda t_1$, the statistical (ensemble) properties of the rainfall intensity in storms of duration D_2 are related to the corresponding statistical properties of the rainfall intensity in storms of duration D_1 according to (7).

It is noted that by setting $\lambda = 1/D$ in (6) we obtain

$$\{\xi(t,D)\} \stackrel{d}{=} \{D^H\xi(t/D,1)\} \tag{10}$$

where $\xi(t/D,1)$ represents the intensity process of a storm event normalized to unit duration. It is then realized from (10) that the hypothesis of scaling implies that the statistical properties of the rainfall intensity in storms of any duration can be obtained by appropriate scaling of the statistical properties of the rainfall intensity in a storm normalized to unit duration.

For reasons of simplicity we will assume that the process $\xi(t,D)$ is stationary within a storm event, i.e., the finite dimensional distribution function is invariant to time translation within a storm,

$$\{\xi(t,D)\} \stackrel{d}{=} \{\xi(t+\tau,D)\}, \quad 0 \le t, t+\tau \le D \tag{11}$$

Note that this is a week stationarity condition in that it represents stationarity of $\xi(t,D)$ only within storm events of a fixed duration and not over any storm, independently of durration, which would imply

$$\{\xi(t)\} \stackrel{d}{=} \{\xi(t+\tau)\} \tag{12}$$

as most available rainfall intensity models, e.g., the Neyman-Scott model, assume. Under our assumption the ensemble statistical properties of the process $\xi(t, D)$ do not depend on t for a given duration D and the ensemble statistical properties of $\xi(t/D, 1)$ are independent of t and D. Let us define as c_1 the ensemble mean of the process $\xi(t/D, 1)$, i.e.,

$$c_1 \equiv E[\xi(t/D, 1)] \tag{13}$$

Since $\xi(t/D, 1)$ is stationary we also define

$$\phi(\tau/D) \equiv E[\xi(t/D, 1)\xi((t+\tau)/D, 1)] \tag{14}$$

Based on the above relations and (6) the ensemble statistical properties of $\xi(t, D)$ can be written as

$$E[\xi(t, D)] = c_1 D^H \tag{15}$$

$$C_\xi(\tau; D) = Cov[\xi(t, D), \xi(t+\tau, D)] = (\phi(\tau/D) - c_1^2)D^{2H} \tag{16}$$

These equations imply that under the hypothesis of simple scaling (equation 6) and the assumption of stationarity within an event (equation 11) the statistical properties of $\xi(t, D)$ can be obtained from the statistical properties of the normalized to unit duration process $\xi(t/D, 1)$ and a scale changing transformation which is a power law of the storm duration. Note that the mean of the rainfall intensity process depend on the duration according to a power law with exponent H, while the covariance of the rainfall intensity process is also a power law of duration with exponent $2H$. Higher product moments follow similar relationships as implied by (10).

4 Properties of total and incremental storm depths

To be able to test the hypothesis of scaling for $\xi(t, D)$ using available rainfall data, the statistical properties of incremental and total storm depths need to be derived. In this section we show that both total storm depths $h(D, D)$ and incremental storm depths $X_\Delta(i, D)$ follow simple scaling laws and expressions for their mean and covariances are derived.

4.1 Cumulative and total storm depths

It can be shown (see Appendix 1) that under some rather mild restrictions on the covariance of $\xi(t, D)$ the cumulative rainfall depth process $h(t, D)$ is also a simple scaling process with exponent $H + 1$, i.e.,

$$\{h(t, D)\} \stackrel{d}{=} \{\lambda^{-(H+1)} h(\lambda t, \lambda D)\} \tag{17}$$

Setting $t = D$ and $\lambda = 1/D$ in the above equation we obtain

$$\{h(D,D)\} \stackrel{d}{=} \{D^{H+1}h(1,1)\} \tag{18}$$

Noting that $E[h(1,1)] = c_1$ and defining

$$c_2 \equiv var[h(1,1)] \tag{19}$$

we can write the ensemble mean and variance of the total storm depth as

$$E[h(D,D)] = c_1 D^{H+1} \tag{20}$$

$$var[h(D,D)] = c_2 D^{2(H+1)} \tag{21}$$

Note that as a result of the simple scaling model for rainfall intensities, the coefficient of variation of the total storm depth is constant and equal to $\sqrt{c_2}/c_1$. Empirical analysis of rainfall data strongly support this property (see Fig. 4 to be discussed later) which, however, is not a property of any stationary model satisfying (12) as it will be discussed in section 6.

4.2 Incremental storm depths

The incremental storm depth at discrete time $t = i$, i.e., $X_\Delta(i,D)$ defined in (2),can be written as the difference of cumulative storm depths as

$$X_\Delta(i,D) = h(i\Delta,D) - h((i-1)\Delta,D) \tag{22}$$

In view of the scaling of $h(t,D)$ (equation 17) the discrete-time incremental depth process $X_\Delta(i,D)$ is also scaling, i.e.,

$$\{X_\Delta(i,D)\} \stackrel{d}{=} \{\lambda^{-(H+1)}X_{\lambda\Delta}(\lambda i,\lambda D)\} \tag{23}$$

It is easy to show that the ensemble mean of $X_\Delta(i,D)$ is

$$E[X_\Delta(i,D)] = c_1\Delta D^H = c_1\delta D^{H+1} \tag{24}$$

where $\delta = \Delta/D$. After some algebraic manipulations one can derive the variance of $X_\Delta(i,D)$ as

$$var[X_\Delta(i,D)] = [\psi(0,\delta) - c_1^2\delta^2]D^{2(H+1)} \tag{25}$$

where

$$\psi(0;\delta) = 2\int_0^\delta \phi(y)(\delta - y)\,dy \tag{26}$$

Similarly , the covariance can be derived as

$$C_{X_\Delta}(m;D) = Cov[X_\Delta(i,D), X_\Delta(i+m,D)] = [\psi(m;\delta) - c_1^2\delta^2]D^{2(H+1)} \tag{27}$$

where

$$\psi(m;\delta) = \int_{(m-1)\delta}^{m\delta}(y-(m-1)\delta)\phi(y)\,dy + \int_{m\delta}^{(m+1)\delta}((m+1)\delta - y)\phi(y)\,dy \quad , m>0 \tag{28}$$

The autocorrelation function can then be written as

$$\rho_{X_\Delta}(m;D) = \frac{\psi(m;\delta) - c_1^2\delta^2}{\psi(0;\delta) - c_1^2\delta^2} \tag{29}$$

It is interesting to note that as a manifestation of the scaling hypothesis for $\xi(t,D)$ the autocorrelation function of the incremental depth process depends on $\delta = \Delta/D$, that is, on the integration interval normalized by the storm duration, and it does not depend directly on the storm duration or the integration interval. The consequence of this is that, for example, $\rho_{X_\Delta}(m;D) = \rho_{X_{2\Delta}}(m;2D)$ which means that the lag-one autocorrelation coefficient of hourly data in a storm of duration D is equal to the lag-one autocorrelation coefficient of two-hour data in a storm of duration $2D$. Since, normally, the autocorrelation increases with the decrease of the lag it follows that the lag-one autocorrelation coefficient of the hourly data in a storm of duration $2D$ is greater than the one of the hourly data in a storm of duration D. Thus the lag-one autocorrelation coefficient is expected to be an increasing function of the storm duration. As it will be seen later the hourly data we analyzed support this property. Another interesting point to note is that the theoretical autocorrelation coefficient of the incremental process is allowed to take on negative values, a property exhibited by hourly rainfall data but not allowed by many stationary models of rainfall intensity as will be discussed in section 6.

5 Model fitting and performance evaluation

5.1 Model fitting procedure

In the previous section the covariance function of $X_\Delta(i,D)$ was derived in terms of the covariance function of $\xi(t,D)$. In order to be able to fit the model to incremental rainfall depths a parametric form for the covariance function of $\xi(t,D)$ must be specified and the covariance of $X_\Delta(i,D)$ must be consequently derived. As it is recalled from (16) the covariance function of $\xi(t,D)$ involves a power function of duration D and a function $\phi(\tau/D)$ of the normalized lag. Here we assume the following power law form for $\phi(y)$

$$\phi(y) = ky^{-\beta} \tag{30}$$

which implies the following power law second product moment for $\xi(t, D)$

$$R_\xi(\tau; D) = kD^{\beta+2H}\tau^{-\beta} \tag{31}$$

Note that this is in contrast to stationary rainfall intensity models for which the above product moment would be a function of lag τ only and not duration.

Based on this and after the computation of the integral in (26) it is shown that

$$C_{X_\Delta}(0; D) = var[X_\Delta(i, D)] = D^{2(H+1)}\delta^2\{2k/[(1-\beta)(2-\beta)]\ \ \delta^{-\beta} - c_1^2\} \tag{32}$$

By considering $C_{X_D}(0; D)$ from the above equation (by setting $\delta = 1$) and equating it to (21) one can see that the parameters k, β of the covariance function of $\xi(t, D)$ are related to c_1 and c_2 by

$$c_2 + c_1^2 = 2k/[(1-\beta)(2-\beta)] \tag{33}$$

By computing the integral in (28) the covariance function of the incremental storm depths is

$$C_{X_\Delta}(m; D) = D^{2(H+1)}\delta^2[(c_2 + c_1^2)\delta^{-\beta}f(m, \beta) - c_1^2], \quad m \geq 0 \tag{34}$$

where

$$f(m, \beta) = [(m-1)^{2-\beta} + (m+1)^{2-\beta}]/2 - m^{2-\beta}, \quad m > 0 \tag{35}$$

and

$$f(0, \beta) = 1 \tag{36}$$

Consequently,

$$\rho_{X_\Delta}(m; D) = \frac{(c_2 + c_1^2)\delta^{-\beta}f(m, \beta) - c_1^2}{(c_2 + c_1^2)\delta^{-\beta} - c_1^2} \tag{37}$$

The model thus has four parameters H, c_1, c_2, and β (note that k is not an independent parameter, since it is related with the others by (33)) which in the empirical analysis that follows were estimated from the following relationships:

$$E[h(D, D)] = c_1 D^{H+1} \tag{38}$$

$$Var[h(D, D)] = c_2 D^{2(H+1)} \tag{39}$$

$$\rho_{X_\Delta}(1; D) = \frac{(1 + c_2/c_1^2)\delta^{-\beta}(2^{1-\beta} - 1) - 1}{(1 + c_2/c_1^2)\delta^{-\beta} - 1} \tag{40}$$

From the first relationship c_1, and H were estimated by least squares and c_2 and β were estimated from the second and third relationship, respectively. Then using (33) the parameter k was obtained. To further evaluate the model performance based on properties not explicitly used for model fitting, the mean, variance, and autocorrelation function of the hourly rainfall depths for storms of different durations were estimated and compared to the theoretical values for the fitted model (equations 24, 32, and 37, respectively).

5.2 Performance evaluation

The data used to test the hypothesis of simple scaling for $\xi(t, D)$ are hourly rainfall depths for a total of 89 storm events of duration greater or equal to two hours. All events occurred during the month of April and during 13 years of record (1971 - 1983) at the Chalara station in the Aliakmon river basin, Greece. Events were identified based on the assumption of independence between events. This amounts to testing for a Poisson process of storm arrivals or exponential distribution for interarrival times. A Kolmogorov-Smirnov test was used for this purpose. Thus events were allowed to include periods of zero rainfall. The maximum zero rainfall period. was found equal to 7 hours The 89 storm events had durations varying from 2 hrs to 49 hrs with a mean duration of 11.8 hrs. General characteristics of the set of storms used are given in Table 1.

To be able to estimate ensemble statistics, the 89 storms were grouped in five classes (1 to 5) according to their duration as shown in Table 2. For example, class 1 includes all 14 storms with duration 2 and 3 hours and class 5 all 17 events with duration between 19 and 45 hours. The basis for selecting this grouping was to have approximately the same number of events in each class. To each class a duration was assigned equal to the mean duration of all events in that class. The events were further grouped into two larger classes (A and B) were class A includes all 39 events of classes 1 and 2 and class B all 36 events of classes 3 and 4. Again the mean duration of each class was used as a representative duration of that class and events in classes A and B were used to estimate the ensemble autocorrelation functions for two different storm durations. The enlarged size was necessary in order to achieve reliable estimations of the autocorrelation coefficients for large lags.

Because there is variability in the durations of the events of each class around the mean duration $\overline{D}$ assigned to that class a correction procedure was applied (when necessary) in estimating the variance of the total depth in each class. This correction consisted of subtracting from the calculated variance the quantity $\sigma_D^2(k_1^2 + k_2^2)$ where σ_D^2 is the variance of the durations in that class and k_1, k_2 are constants obtained from the linearization of the mean and standard deviation of total depths, respectively, in the neighborhoud of $\overline{D}$, i.e, $E[h(D, D)] \approx k_1\overline{D}$ and $\{Var[h(D, D)]\}^{1/2} \approx k_2\overline{D}$ For the scaling process we have $c_1\overline{D}^{H+1} \approx k_1\overline{D}$ and $c_2\overline{D}^{2(H+1)} \approx k_2^2\overline{D}^2$ and thus the correction applied was

$$\sigma_D^2(c_1^2 + c_2)\overline{D}^{2H} \tag{41}$$

It was found that this correction was negligible for all classes except the class with the larger durations (class 5). The necessity of such a correction implies an iterative process for the estimation of c_2.

Based on the parameter estimation procedure discussed in the previous section the following

parameter estimates were obtained for this data set:

$$\hat{H} = -0.20, \quad \hat{c}_1 = 1.05, \quad \hat{c}_2 = 0.44, \quad \hat{\beta} = 0.32 \tag{42}$$

For these parameters the value of $k = 0.88$.

The empirical means and standard deviations of total storm depths as a function of duration as well as the theoretical curves from the fitted model are shown in Figure 3. Fig. 4 shows the empirical coefficients of variation of the total storm depth which is almost independent of duration and the theoretical coefficient of variation which is constant and equal to $\sqrt{c_2}/c_1 = 0.63$. The empirical and theoretical lag one autocorrelation coefficents of hourly rainfall depths are shown in Fig. 5 as a function of storm duration. Although deviations between the empirical and theoretical values are observed when 90% approximate confidence intervals (computed by using the Fisher transformation for the autocorrelation coefficient) were positioned around the empirical values only 1 of the 5 values was outside the confidence intervals as statistically expected.

To check the performance of the model we computed the empirical and theoretical mean and standard deviation of the hourly rainfall depths for different durations (shown in Fig. 6) and the autocorrelation functions for classes A and B (shown in Fig. 7). It is seen that the scaling model performs reasonably well in terms of capturing statistical properties of total and incremental storm depths in storms of different durations. The largest deviation between the empirical and theoretical statistics are found for storms of only two hours duration (see, for example, Fig. 6).

6 Comparison with stationary models

In this section we derive the statistical properties of total and incremental storm depths for two simple stationary models, i.e., models satisfying (12) and demonstrate both analytically and empirically that these models are not able to capture important statistical characteristics of storm rainfall that the simple scaling model is able to capture.

6.1 Derivation of statistical properties

It is easy to see that

$$E[h(D, D)] = E[h(D)] = c_1 D \tag{43}$$

$$E[X_\Delta(i, D)] = E[X_\Delta(i)] = c_1 \Delta \tag{44}$$

where $c_1 = E[\xi(t, D)] = E[\xi(t)]$. To derive the expressions for the variance and covariance of $h(D)$ and $X_\Delta(i)$ we need to specify functional forms for the autocorrelation function of $\xi(t)$. The

following two common models (power law and markovian) are examined:

$$Model\ 1: \quad C_\xi(\tau, D) = C_\xi(\tau) = k_1 \tau^{-\beta_1} \tag{45}$$

$$Model\ 2: \quad C_\xi(\tau, D) = C_\xi(\tau) = k_2 e^{-\beta_2 \tau} \tag{46}$$

After algebraic manipulations it can be shown that for model 1

$$Var[h(D)] = \frac{2k_1}{(1-\beta_1)(2-\beta_1)} D^{2-\beta_1} \tag{47}$$

$$Var[X_\Delta(i)] = \frac{2k_1}{(1-\beta_1)(2-\beta_1)} \Delta^{2-\beta_1} \tag{48}$$

$$\rho_{X_\Delta}(m) = \frac{1}{2}[(m-1)^{2-\beta_1} + (m+1)^{2-\beta_1}] - m^{2-\beta_1} \tag{49}$$

and for model 2

$$Var[h(D)] = 2(k_2^2/\beta_2^2)(\beta_2 D - 1 + e^{-\beta_2 D}) \tag{50}$$

$$Var[X_\Delta(i)] = 2(k_2^2/\beta_2^2)(\beta_2 \Delta - 1 + e^{-\beta_2 \Delta}) \tag{51}$$

$$\rho_{X_\Delta}(m) = \frac{(1-e^{-\beta_2\Delta})^2}{2(\beta_2\Delta - 1 + e^{-\beta_2\Delta})} e^{-\beta_2(m-1)\Delta}) \tag{52}$$

Note that in both of the above models the coefficient of variation of the total storm depth is not constant but is a function of the storm duration. For example, for model 1 the coefficient of variation is $(\sqrt{2k_1/[(1-\beta_1)(2-\beta_1]}/c_1)D^{-\beta_1/2}$. This property of the model is in disagreement with the empirical evidence (see Fig. 9) that the coefficient of variation of total strom depths is constant and independent of storm duration.

In the next section these two models are fitted to the data from the 89 storms described earlier.

6.2 Model fitting and performance evaluation

Both models have three parameters. Equation (43) can be used to estimate c_1 using the sample of total depths. Equations (49) and (52), when setting $m = 1$, can be used to estimate β_1 and β_2, respectively. The empirical lag-one autocorrelation coefficient used in these equations can be calculated from the whole sample of hourly data. Finally k_1 and k_2 are estimated from equations (48) and (51), respectively, by using the sample of total depths. The following parameters were estimated for the above two models:

$$\begin{aligned} &Model\ 1: \hat{c}_1 = 0.65, \quad \hat{k}_1 = 0.61, \quad \hat{\beta}_1 = 0.51 \\ &Model\ 2: \hat{c}_1 = 0.65, \quad \hat{k}_2 = 1.25, \quad \hat{\beta}_2 = 1.58 \end{aligned} \tag{53}$$

Fig. 8 shows the empirical and theoretical mean and standard deviation of the total storm depths. It is observed that both stationary models are not able to capture the duration dependent structure of these statistics. This is further verified by Fig. 9 which shows the empirical and theoretical coefficient of variation of the total storm depths as a function of duration. The empirical and theoretical first autocorrelation coefficient of the hourly rainfall depths is shown in Fig. 10 as a function of duration. As was analytically seen from (49) and (52) the autocorrelation of hourly rainfall depths is independent of the duration and cannot obtain negative values This is in disagreement with the empirical observations (see, for example, Fig. 10).

To further evaluate the model performance based on properties not explicitly used in model fitting we evaluated the empirical and theoretical mean and standard deviation of the hourly rainfall depths (equations 44, 48, and 51) and autocorrelation functions (equations 49 and 52) for model 1 and model 2, respectively. These figures together with Figs. 8, 9, and 10 demonstrate the superiority of the scaling model and the inability of the stationary model to capture important statistical properties of storm rainfall.

7 Mass curves

The use of dimensionless mass curves, i.e., normalized rainfall depth $h^*(t/D)$ versus normalized time t/D, implies that a stochastic function $h^*(.)$ can be found such that

$$h(t,D) = h^*(t/D)h(D,D) \tag{54}$$

where $h^*(t/D)$ is a stochastic function independent of D and $h(D,D)$ is a stochastic variable independent of t. Taking k moments of the above equation we obtain

$$E[h(t,D)^k] = E[h^*(t/D)^k]E[h(D,D)^k] \tag{55}$$

It is easy to show that under the assumption of stationarity over time (12) no function $h^*(t/D)$ can be found such that (55) is satisfied for all k while under the assumption of scaling and stationarity within storms (11) such a function exists. Consider, for example, model 1 for which

$$E[h(t,D)] = c_1 t = c_1(t/D)D \tag{56}$$

and

$$\begin{aligned} E[h(t,D)^2] &= c_1^2 t^2 \; + \; \{2k_1/[(1-\beta_1)(2-\beta_1]\}t^{2-\beta} \\ &= c_1^2(t/D)^2 D^2 \; + \; \{2k_1/[(1-\beta_1)(2-\beta_1]\}\; (t/D)^{2-\beta} D^{2-\beta} \end{aligned} \tag{57}$$

It becomes apparent that for k =2 no function $h^*(t/D)$ can be found to satisfy (55). At the same time, for the simple scaling model

$$E[h(t,D)^k] = D^{k(H+1)} E[h(t/D,1)^k] \tag{58}$$

which is consistent with (55)

We conclude that the proposed simple scaling model is consistent with the concept and use of mass curves while any stationary model is not.

References

[1] Huff, F. A., Time distribution of rainfall in heavy storms, *Water Resour. Res.*, 3(4), 1007-1019, 1967.

[2] Lamperti, J., Semi-Stable Stochastic Processes, *Trans. Amer. Math. Soc.*, Vol. 104, p. 62-78, 1962.

[3] Pilgrim, D. H. and I. Cordery, Rainfall temporal patterns for design floods, *J. Hydr. Div., ASCE*, 101(HY1), 81-95, 1975.

[4] Rodriguez-Iturbe I., Gupta, V.K. and Waymire, E. Scale considerations in the modeling of temporal rainfall *Water Resour. Res.*, 20(11), 1611-1619, 1984.

8 Appendix 1: Self-similarity of $h(t, D)$

Let us consider the (k, ℓ) second product moment of $h(t, D)$

$$\begin{aligned} & E\{h(t_1, D)^k h(t_2, D)^\ell\} \\ &= E\{[\int_0^{t_1} \xi(s, D)\, ds]^k [\int_0^{t_2} \xi(q, D)\, dq]^\ell\} \\ &= \int_0^{t_1} \cdots \int_0^{t_1} \int_0^{t_2} \cdots \int_0^{t_2} E\{\xi(s_1, D) \cdots \xi(s_k, D) \xi(q_1, D) \cdots \xi(q_\ell, D)\} \\ & \qquad\qquad ds_1 \cdots ds_k\, dq_1 \cdots dq_\ell \end{aligned} \tag{59}$$

Similarly,

$$\begin{aligned} & E\{h(\lambda t_1, \lambda D)^k h(\lambda t_2, \lambda D)^\ell\} \\ &= \int_0^{\lambda t_1} \cdots \int_0^{\lambda t_1} \int_0^{\lambda t_2} \cdots \int_0^{\lambda t_2} E\{\xi(s_1, \lambda D) \cdots \xi(s_k, \lambda D) \xi(q_1, \lambda D) \cdots \xi(q_\ell, \lambda D)\} \\ & \qquad\qquad ds_1 \cdots ds_k\, dq_1 \cdots dq_\ell \\ &= \int_0^{t_1} \cdots \int_0^{t_1} \int_0^{t_2} \cdots \int_0^{t_2} E\{\xi(\lambda\sigma_1, \lambda D) \cdots \xi(\lambda\sigma_k, \lambda D) \xi(\lambda\psi_1, \lambda D) \cdots \xi(\lambda\psi_\ell, \lambda D)\} \lambda^{k+\ell} \\ & \qquad\qquad d\sigma_1 \cdots d\sigma_k\, d\psi_1 \cdots d\psi_\ell \end{aligned} \tag{60}$$

where the last equality has been obtained by setting $s_i = \lambda\sigma_i$ and $q_i = \lambda\psi_i$. Note that this last equality would not hold if any product moment contained dirac delta terms. This can be seen by considering for simplicity one term only, say $E[\xi(s, \lambda D)]$, and observing that if that term had the form $f(s)\delta(s - s_0)$ then $\int_0^{\lambda t} E[\xi(s, \lambda D)]\, ds = \int_0^{\lambda t} f(s)\delta(s - s_0)\, ds = f(s_0)$ while the term obtained by substituting $s = \lambda\sigma$ would give $\int_0^t E[\xi(\lambda\sigma, \lambda D)]\lambda\, d\sigma = \int_0^t f(\lambda\sigma)\delta(\lambda\sigma - s_0)\lambda\, d\sigma = \lambda f(s_0) \neq f(s_0)$.

In view of (9) the above equality can be further written as

$$\begin{aligned} & E\{h(\lambda t_1, \lambda D)^k h(\lambda t_2, \lambda D)^\ell\} \\ &= \lambda^{k+\ell} \lambda^{H(k+\ell)} \int_0^{t_1} \cdots \int_0^{t_1} \int_0^{t_2} \cdots \int_0^{t_2} E\{\xi(\lambda\sigma_1, \lambda D) \cdots \xi(\lambda\sigma_k, \lambda D) \xi(\lambda\psi_1, \lambda D) \cdots \xi(\lambda\psi_\ell, \lambda D)\} \\ & \qquad\qquad d\sigma_1 \cdots d\sigma_k\, d\psi_1 \cdots d\psi_\ell \end{aligned} \tag{61}$$

By comparing (59) and (61) we obtain

$$\lambda^{-(H+1)(k+\ell)} E\{h(\lambda t_1, \lambda D)^k h(\lambda t_2, \lambda D)^\ell\} = E\{h(t_1, D)^k h(t_2, D)^\ell\} \tag{62}$$

This result can be similarly extended to the product moments of any order and thus we conclude that

$$\{h(t, D)\} \stackrel{d}{=} \{\lambda^{-(H+1)} h(\lambda t, \lambda D)\} \tag{63}$$

List of Tables

List of Figures

	Min	Max	Mean	Std
Duration (h)	2	45	11.8	8.9
Interarrival time (h)	10	470	101.3	106.2
Total depth (mm)	0.3	38.9	7.5	7.7
Mean intensity (mm/h)	0.1	2.55	0.69	0.48
Hourly depth (mm)	0.0	8.2	0.64	0.93

Table 1: General characteristics of the 89 storms used in the analysis.

class	D_{min}	D_{max}	$\overline{D}$	σ_D	No. of events N_1	Total no. of hourly depths N_2
1	2	3	2.2	0.4	14	31
2	4	7	5.4	1.2	20	108
3	8	11	9.7	1.1	19	184
4	12	18	14.2	1.9	19	269
5	19	45	27.1	6.2	17	461
A=(2+3)	4	11	7.4	2.4	39	292
B=(4+5)	12	45	20.3	7.9	36	730
Total	2	45	11.8	8.9	89	1053

Table 2: Classification of storms according to their duration. The storms in each class were used to estimate the ensemble statistics of that class.

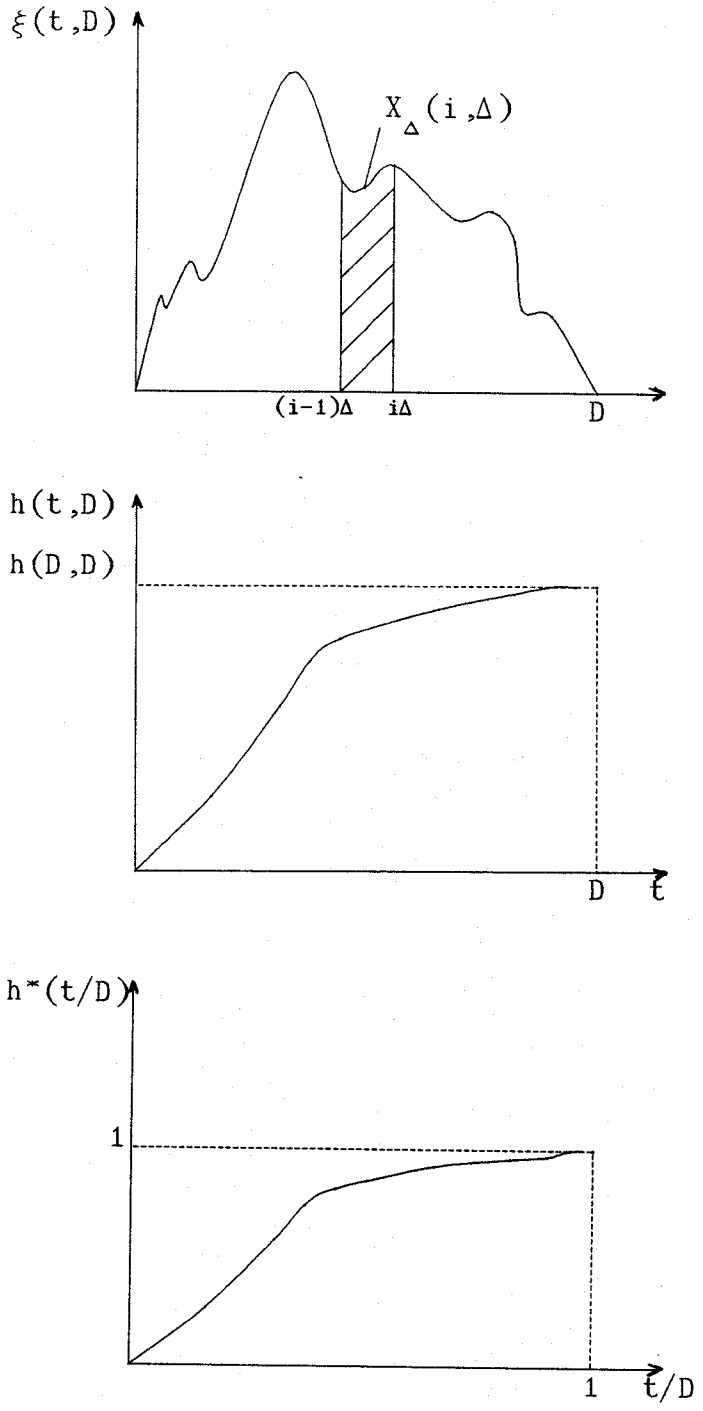

Figure 1: Definition of terms.

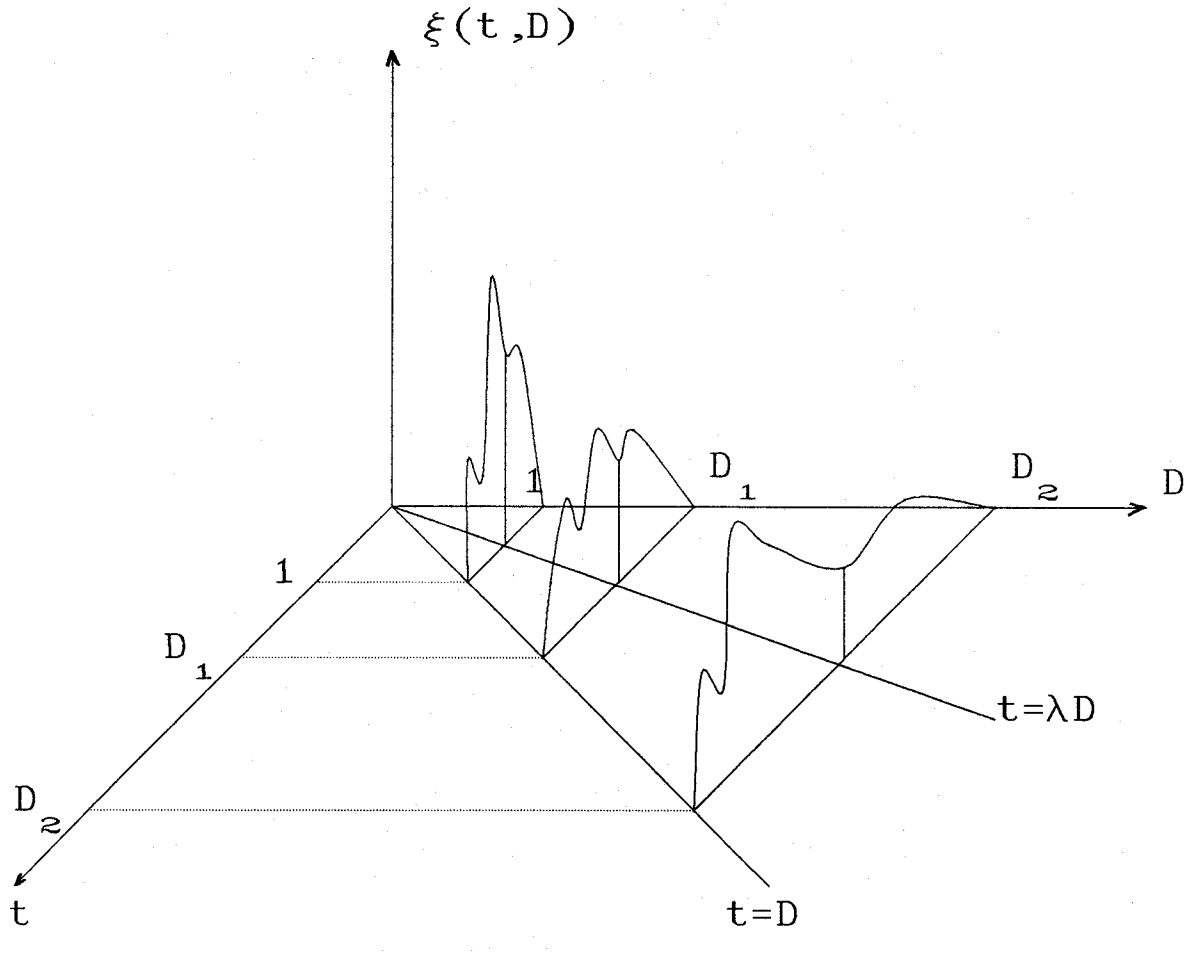

Figure 2: Schematic for explanation of scaling.

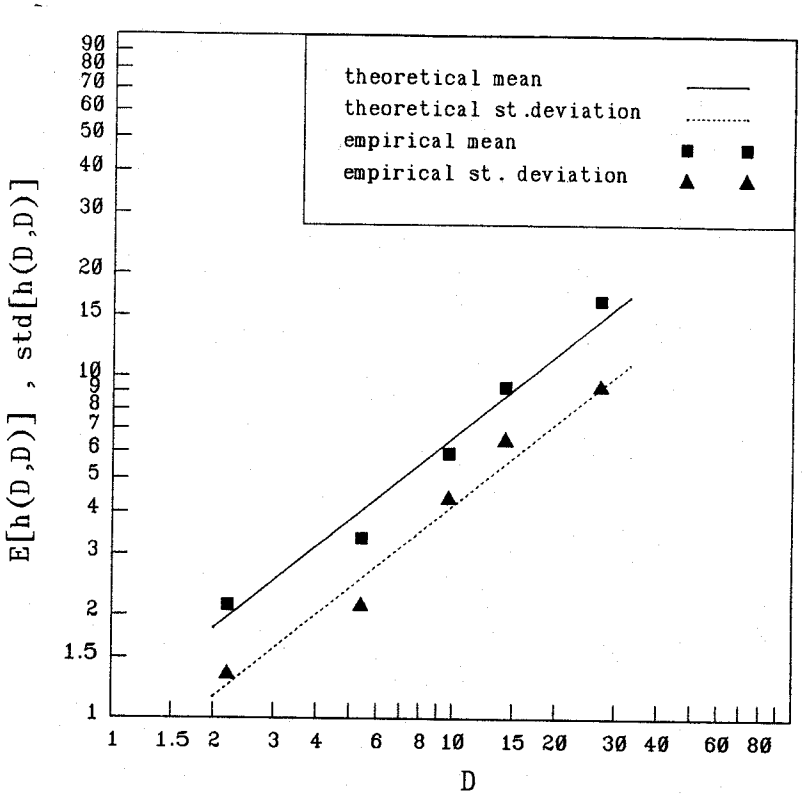

Figure 3: Scaling model: empirical and theoretical means and standard deviations of total storm depths as a function of storm duration (log-log plot).

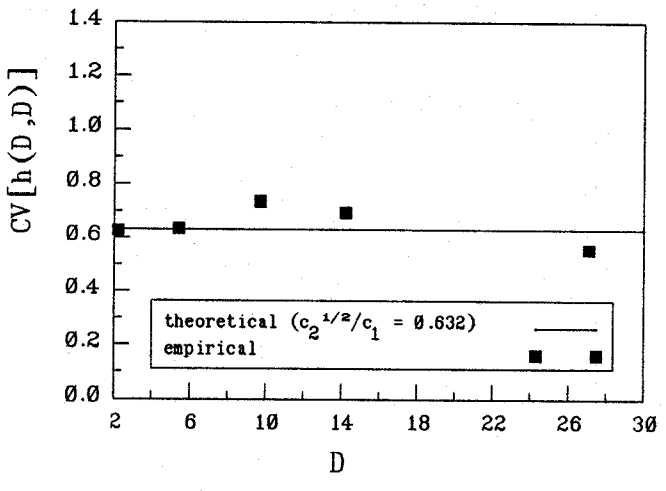

Figure 4: Scaling model: empirical and theoretical coefficient of variation of total storm depths as a function of duration.

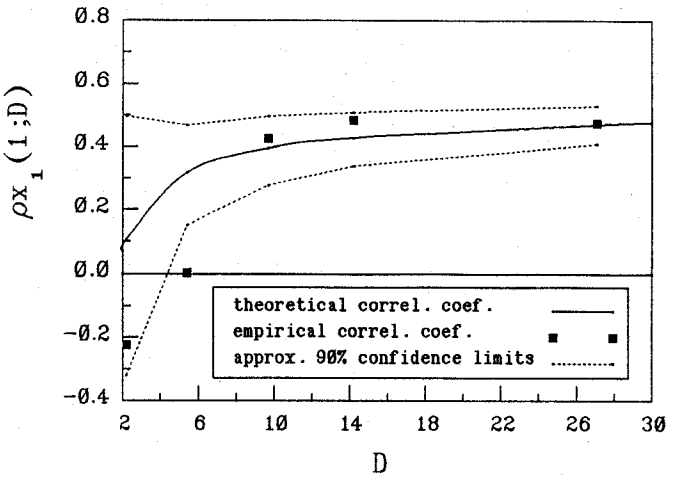

Figure 5: Scaling model: empirical and theoretical first autocorrelation coefficient of hourly rainfall depths as a function of duration.

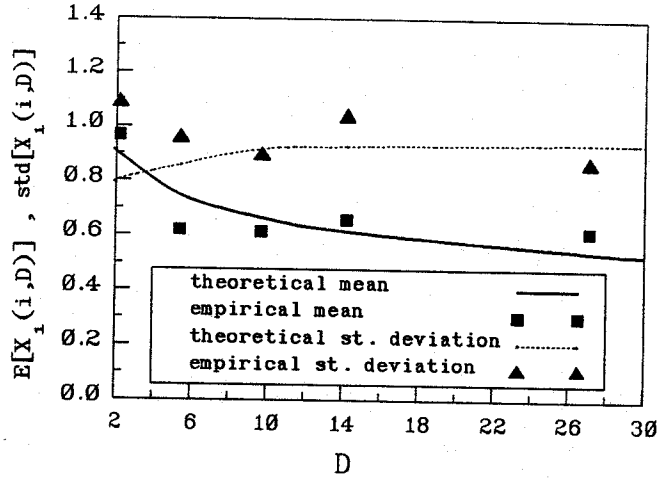

Figure 6: Scaling model: empirical and theoretical mean and standard deviation of hourly rainfall depths as a function of duration.

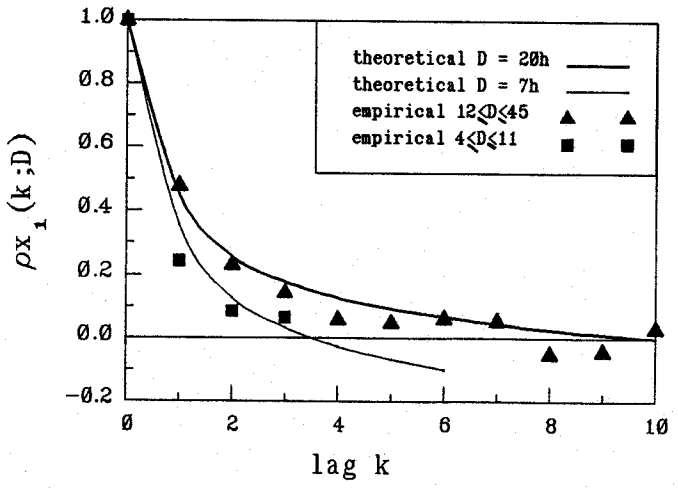

Figure 7: Scaling model: empirical and theoretical autocorrelation function of hourly rainfall depths as a function of duration.

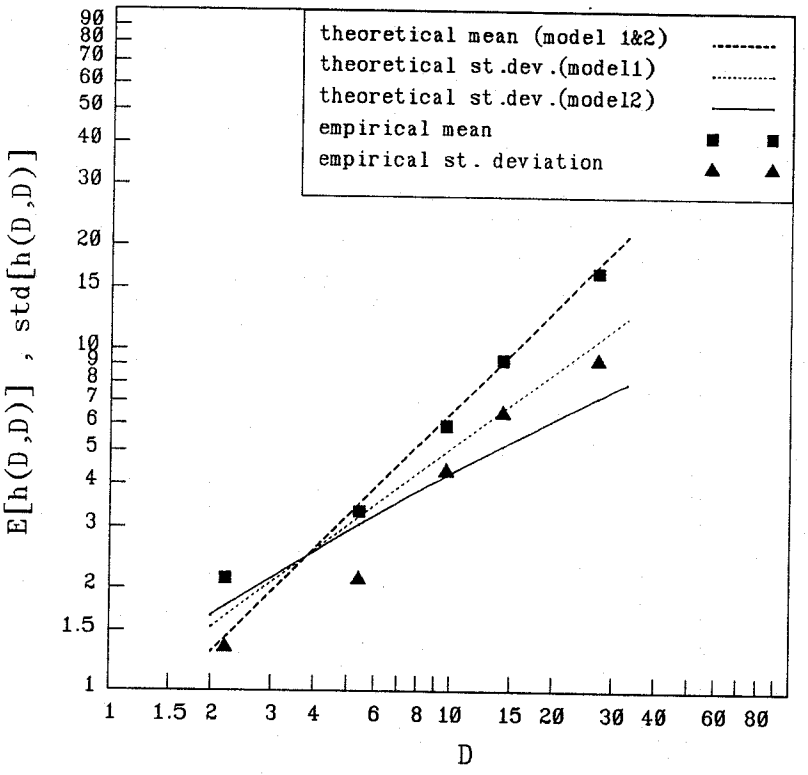

Figure 8: Stationary models: empirical and theoretical means and standard deviations of total storm depths as a function of storm duration (log-log plot).

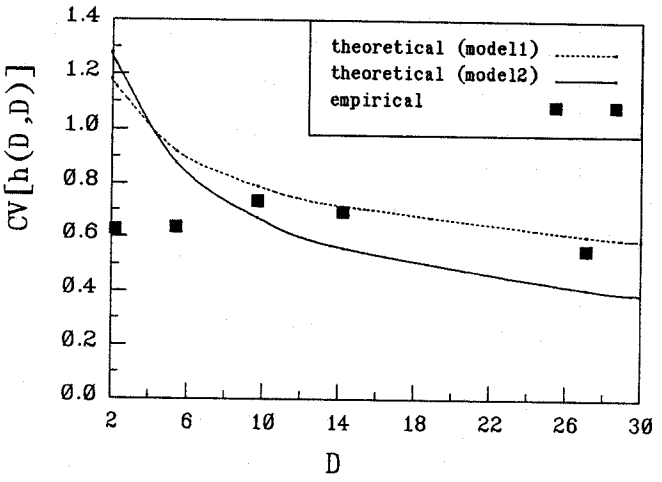

Figure 9: Stationary models: empirical and theoretical coefficient of variation of total storm depths as a function of duration.

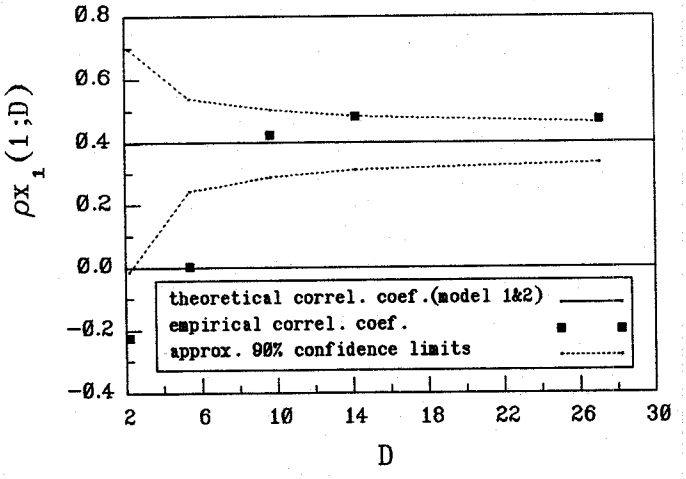

Figure 10: Stationary models: empirical and theoretical first autocorrelation coefficient of hourly rainfall depths as a function of duration.

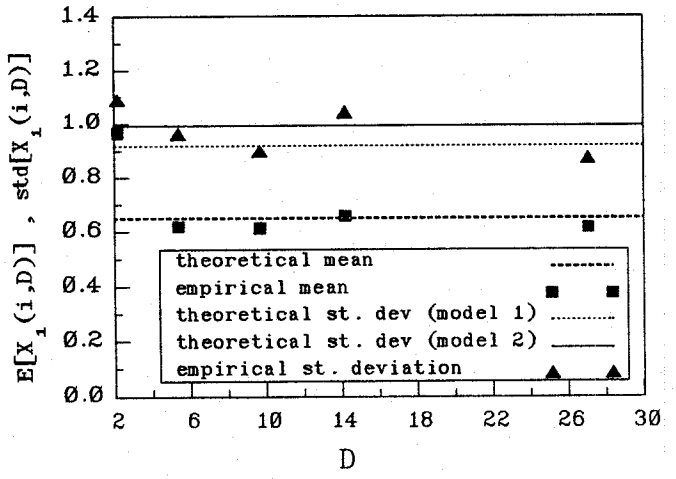

Figure 11: Stationary models: empirical and theoretical mean and standard deviation of hourly rainfall depths as a function of duration.

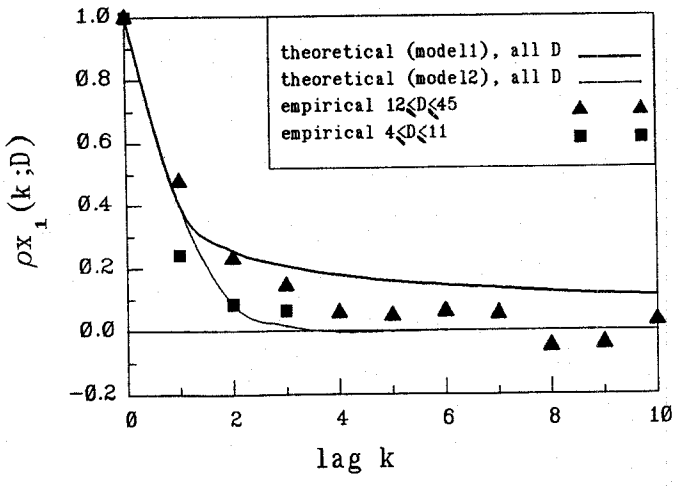

Figure 12: Stationary models: empirical and theoretical autocorrelation function of hourly rainfall depths as a function of duration.